Spatiotemporal Evolution and Multiscale Spatial Heterogeneity of Coupled and Coordinated Development Between Agriculture and Ecological Environment in China

Zebin Liu[1], Tesfaye Haile[2]*, Wanxue Chen[1]

[1]*Huainan Normal University, Dongshan Road Street, Huainan, 232000, China*

[2]*Temple University, North Broad Street, Philadelphia,19121, United States*

* All correspondence should be addressed: e-mail: tesfayehaile182@gmail.com

11 Graphical abstract

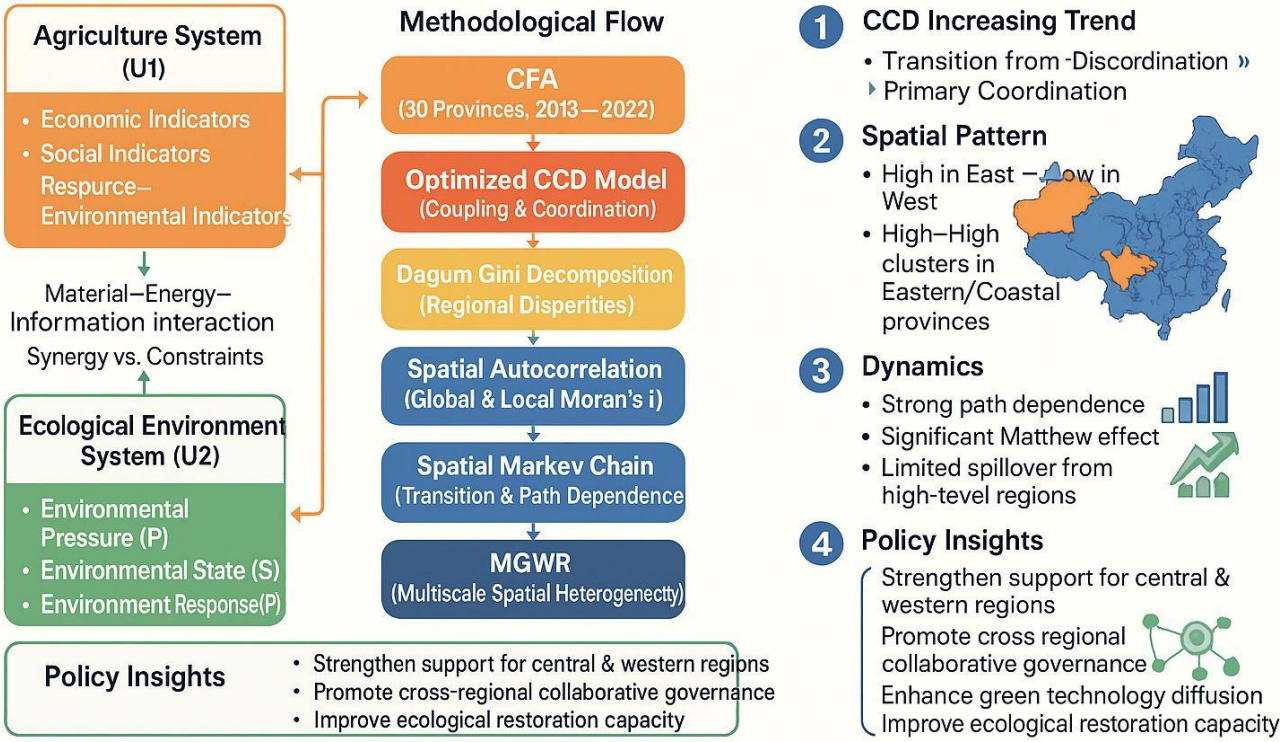

12

Abstract

Against the backdrop of Chinese-style modernization and the national "dual-carbon" goals, clarifying the coupling and coordination relationship between agricultural development and ecological environmental protection is of great significance for safeguarding food and ecological security and advancing rural revitalization. Based on panel data from 30 Chinese provinces from 2013 to 2022, this paper constructs an evaluation index system for the two subsystems of agricultural development and the ecological environment, and employs confirmatory factor analysis to derive comprehensive development indices. On this basis, a coupling coordination degree (CCD) model is developed and optimized. The study further incorporates the Dagum Gini coefficient and its decomposition, global and local Moran's I, kernel density estimation, spatial Markov chains, and multi-scale geographically weighted regression (MGWR) to systematically depict the spatio-temporal evolution and multi-scale spatial non-stationarity of the coupling and coordinated development between the two systems. The results indicate that the national CCD has increased overall, shifting from a state of maladjustment to a stage of primary coordination. A spatial pattern characterized by "higher in the east and lower in the west" and by "high–high" and "low–low" clusters has emerged. Regional disparities are mainly driven by an east–west divide, and path dependence as well as a pronounced "Matthew effect" are observed. The scale of the agricultural economy, the level of regional development, infrastructure, investment in ecological governance, and the quality of the ecological environment all significantly promote coupling and coordination, although their effects display marked spatial heterogeneity. Accordingly, it is necessary to implement region-specific and category-specific policies and to strengthen cross-regional collaborative governance.

Keywords: agriculture, ecological environment, coupling coordination degree, spatiotemporal analysis, regional heterogeneity; sustainable regional development

1.Introduction

Achieving synergy between high-quality agricultural development and high-level ecological environmental protection is a critical issue for advancing Chinese-style modernization, realizing the "dual-carbon" (carbon peaking and carbon neutrality) goals, and implementing the rural revitalization strategy(Han et al., 2024;Wu et al., 2024). On the one hand, agriculture is highly dependent on natural resources, climatic conditions, and ecosystem services—such as water conservation, soil retention, and biodiversity maintenance(Cheng et al., 2022;Power, 2010). On the other hand, agricultural production significantly affects environmental quality through multiple pathways, including the use of chemical fertilizers and pesticides, surface runoff and non-point source pollution, straw management practices, and greenhouse gas emissions(Liang et al., 2021). Consequently, the interaction between the agricultural and ecological environment systems embodies both coupling effects that promote coordinated development and trade-offs that may constrain it(Liu et al., 2025). The spatiotemporal evolution and regional heterogeneity of this system's co-development trajectory are directly linked to food security, ecological security, and regional sustainability.

Current research on agriculture and the ecological environment primarily follows two threads. The first concerns the construction of measurement and evaluation systems. In this area, indicator frameworks for agricultural green development and ecological environment quality have become relatively mature. Most studies construct agricultural development and ecological environment indices using methods such as the entropy method(Wan et al., 2023;Tang et al., 2022;Liu et al., 2020), the coefficient of variation(Qiu et al., 2021), or hybrid subjective–objective approaches(Chen et al., 2022) (e.g., Analytic Hierarchy Process (AHP) × entropy, CRITIC × TOPSIS), and employ these indices to assess the development quality of the two domains. The second research strand focuses on the mechanisms underlying their interrelationship. Scholars have concentrated on two major sets of

mechanisms. The first pertains to the pressure exerted on the environment by agricultural intensification(Kopittke et al., 2019), notably nutrient pollution(Madjar et al., 2024), greenhouse gas emissions(Smith et al., 2008), land-use change(Gallardo, 2024), and biodiversity loss(Raven et al., 2021). The second concerns the supporting role of ecosystem services for agricultural production and the risks arising from their degradation, including pollination and biological pest control(Lundin et al., 2013), landscape-pattern regulation(Bianchi et al., 2006), and climate and environmental constraints(Hu et al., 2024). In addition, a body of work approaches the coordination of agricultural green development and ecological protection from policy and institutional perspectives: on the one hand, emphasizing ecological priorities(Huo et al., 2025) and proposing strategies to steer agricultural industrial systems toward green transformation(Zhao et al., 2022); on the other hand, examining rural ecological compensation mechanisms and policy mixes designed to achieve synergies between ecological protection and modern agricultural development(He, 2019;Luo, 2023).

Although the literature on this topic is abundant, studies that examine the agriculture–environment relationship from a coupling–coordination perspective remain relatively scarce. Three specific shortcomings can be identified. First, the prevailing research paradigm emphasizes static measurement and lacks in-depth analysis of the dynamic evolution of coupling and coordination. Second, many studies focus on unidirectional impact mechanisms and therefore fail to systematically identify bidirectional coupling and feedback effects. Third, much of the literature is framed as macro-level policy discussion and lacks empirical evidence for identifying coordinated optimization pathways under conditions of spatial heterogeneity. To address these gaps, this paper uses a panel of 30 Chinese provinces for the period 2013–2022 and proceeds from two subsystems—agricultural development and the ecological environment. A composite development index is extracted via Confirmatory Factor Analysis (CFA). On this basis, we measure and optimize a coupling coordination

degree (CCD) model to improve robustness to extreme values and enhance sensitivity to relative differences. Methodologically, the study combines global and local spatial analysis techniques. Global and local Moran's I statistics and hotspot detection are used to reveal spatial dependence and clustering patterns. Kernel density estimation is employed to depict distributional dynamics and polarization trends. A spatial Markov chain framework characterizes the transition processes and steady-state features of coordination states in neighborhood contexts. Finally, multiscale geographically weighted regression (MGWR) is introduced to identify spatial nonstationarity in drivers and the action scales associated with each variable. Based on the above framework, this study seeks to answer the following questions: (1) During 2013–2022, what stages did the coupling–coordination level between agriculture and the ecological environment in Chinese provinces occupy, and what temporal trends did it exhibit? (2) Does the level of coordination display significant positive spatial correlation and clustering? (3) Under spatial neighborhood influences, do transitions in coordination states exhibit path dependence and a "Matthew effect"? (4) How do the key drivers of coupled evolution vary across regions in terms of multiscale heterogeneity?

The marginal contributions of this paper are reflected in three main aspects. First, at the methodological level, this study refines the conventional CCD model by directly measuring subsystem disparities and introducing a logarithmic–exponential transformation. These improvements enhance the model's robustness and explanatory power, thereby capturing more accurately the intrinsic "synergy–tension" relationship between agricultural development and the ecological environment. Second, at the spatiotemporal mechanism level, the study systematically reveals the temporal evolution, spatial agglomeration, differentiation, and path dependence of coordination levels. This provides empirical evidence for understanding the interregional "spillover–lock-in" mechanisms that characterize the coevolution of agriculture and the ecological environment.

Third, at the heterogeneity identification level, the paper uncovers differentiated pathways across regions shaped by variations in ecological endowment, industrial structure, and factor inputs. On this basis, it proposes region-specific and classification-based strategies for precision governance and policy design tailored to local conditions.

2. Theoretical analysis of the coupling coordination mechanism

The coupled and coordinated development between agriculture and the ecological environment constitutes a complex adaptive system driven by the co-evolution of socio-economic activities and biophysical constraints (Figure1). To clarify the internal logic of this system, we frame the coupling mechanism through four interactive dimensions: resource–environment coupling (the foundation), green agglomeration and innovation (the driver), spatial interaction (the amplifier), and policy regulation (the stabilizer). This relationship transcends a simple linear interaction; it is characterized by dynamic feedback loops, threshold effects, and spatial spillovers that jointly shape the spatiotemporal evolution of the CCD. Fundamentally, the coupling mechanism operates through the exchange of material, energy, and information flows, where the agricultural system relies on ecosystem services (e.g., soil retention, water conservation) while simultaneously exerting pressure on these systems through resource extraction and emissions.

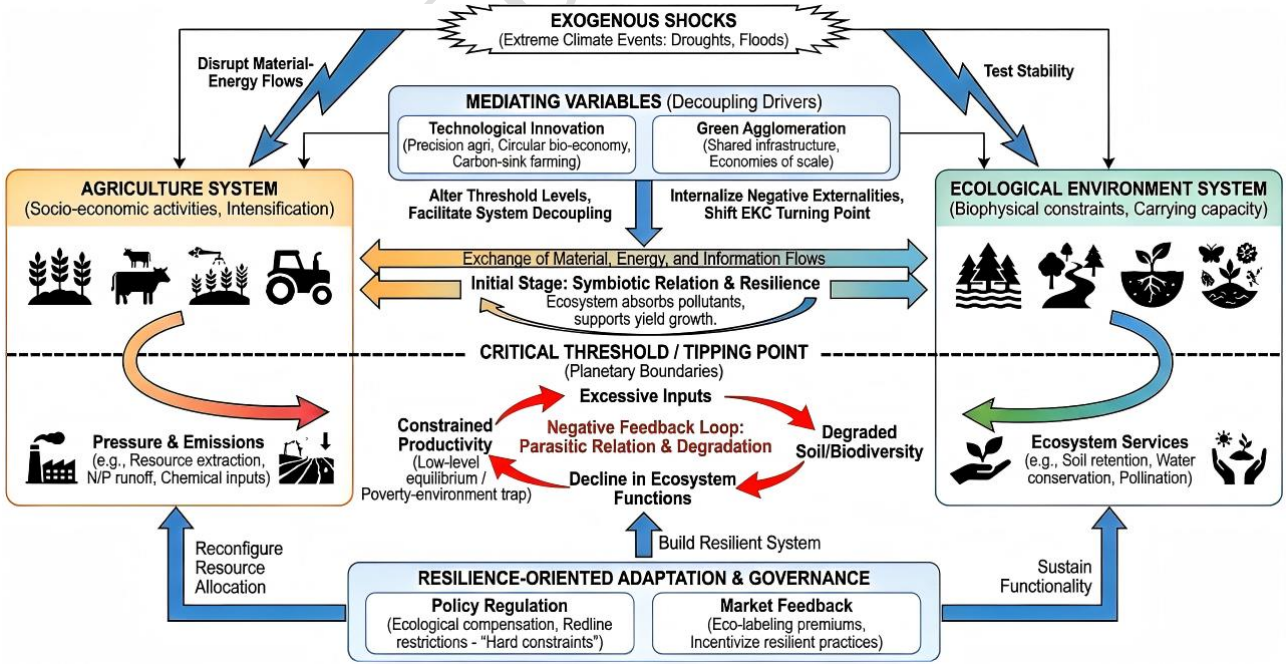

Figure1. Coupling and coordination mechanism between agriculture and ecological environment

First, regarding the dimension of resource-environment coupling, the coordination between

agricultural intensification and environmental carrying capacity exhibits distinct non-linear threshold effects and feedback mechanisms(Watson et al., 2021). In the initial stage of development, the ecosystem possesses a certain resilience, allowing it to absorb agricultural pollutants (e.g., nitrogen and phosphorus runoff) and support yield growth. However, once resource extraction and pollution intensity exceed critical "tipping points"—akin to planetary boundaries—the relationship shifts from symbiotic to parasitic(Rockström et al., 2023). This triggers a negative feedback loop: excessive use of chemical inputs degrades soil structure and biodiversity, leading to a decline in ecosystem service functions (such as pollination and pest control). This degradation subsequently acts as a binding constraint on agricultural productivity, potentially trapping the system in a "low-level equilibrium" or a “poverty-environment trap” where higher inputs yield diminishing marginal returns(Burian et al., 2024).

Second, in terms of green agglomeration and innovation, these factors serve as critical mediating variables that can alter these threshold levels and facilitate system decoupling. The diffusion of green technologies—such as precision agriculture, circular bio-economy practices, and carbon-sink farming—modifies the elasticity of substitution between natural capital and man-made capital. However, technical solutions alone are insufficient; recent scholarship emphasizes that human capital serves as a vital moderating variable, ensuring that environmental technologies are effectively adopted and translated into coordination gains(Lei et al., 2026b). By internalizing negative externalities (e.g., through waste-to-energy recycling or biological pest control), technological innovation shifts the Environmental Kuznets Curve (EKC) turning point, allowing for agricultural economic growth without a proportional increase in environmental degradation. Furthermore, spatial agglomeration generates economies of scale in pollution abatement, though evidence suggests that peer effects in abnormal R&D intensity can deteriorate innovation quality, implying that high-quality coordination requires avoiding "blind competition" in factor inputs(Lei et al., 2026a).

Third, concerning policy regulation and spatial interaction, the stability of this coupling is increasingly tested by exogenous shocks, particularly extreme climate events, which necessitate a shift from purely efficiency-oriented coordination to resilience-oriented adaptation. Climate change introduces volatility into the coupling mechanism; for instance, typhoon shocks have been found to significantly reduce R&D activities, disrupting the innovation systems necessary for agricultural adaptation(Lei et al., 2024). Under these conditions, the coupling mechanism relies on responsive policy regulation and market feedback to reconfigure resource allocation. Yet, policy interventions

must be context-sensitive, as well-intentioned cleaner production mandates can generate unintended negative outcomes if implementation contexts are not adequately considered (Lei et al., 2025). Consequently, high-quality coordinated development is achieved not merely by minimizing environmental impact, but by building a resilient system capable of absorbing shocks and sustaining functionality through adaptive governance to mitigate the negative externalities of spatial interactions.

Based on the theoretical mechanism analysis above, specifically the existence of threshold effects, spatial spillovers, and regional heterogeneity in factor endowments, this paper proposes the following three research hypotheses to guide the empirical analysis:

(1) Hypothesis 1 (H1): Driven by the "decoupling" mechanism of technological innovation and structural upgrading, the CCD between agriculture and the ecological environment will show an upward trend, but due to the constraints of initial endowments (resource-environment coupling thresholds), the evolution process will exhibit significant path dependence.

(2) Hypothesis 2 (H2): Due to the cross-regional mobility of ecosystem services and economic factors (spatial interaction), the CCD is not spatially random but exhibits significant positive spatial correlation; under the influence of the "siphon effect" from advanced regions, the spatial pattern will demonstrate a "Matthew Effect" (high-high and low-low clustering).

(3) Hypothesis 3 (H3): Influenced by the differing development stages and ecological carrying capacities across regions, the driving factors (e.g., economic scale, infrastructure, ecological quality) exert spatially non-stationary impacts on the CCD, resulting in significant multiscale spatial heterogeneity in their marginal effects.

3. Indicators Construction

This study utilizes panel data from 2013 to 2022 covering 30 provincial-level administrative divisions in mainland China. To ensure that the analysis of spatial heterogeneity is rigorous and replicable, the research sample is strictly divided into four economic regions following the standard classification of the National Bureau of Statistics (2011): the Eastern Region includes 10 provinces and municipalities (Beijing, Tianjin, Hebei, Shanghai, Jiangsu, Zhejiang, Fujian, Shandong, Guangdong, Hainan) characterized by advanced modernization; the Central Region comprises 6 provinces (Shanxi, Anhui, Jiangxi, Henan, Hubei, Hunan); the Western Region covers 11 provinces

and autonomous regions (Inner Mongolia, Guangxi, Chongqing, Sichuan, Guizhou, Yunnan, Shaanxi, Gansu, Qinghai, Ningxia, Xinjiang); and the Northeastern Region consists of 3 provinces (Liaoning, Jilin, Heilongjiang). Regarding sample selection, the Tibet Autonomous Region, as well as Hong Kong, Macao, and Taiwan (HKMT), are excluded from the empirical analysis. This exclusion is justified on two grounds: First, statistical inconsistency and data availability. The statistical accounting standards in HKMT differ significantly from those in mainland China (e.g., distinct definitions of agricultural inputs and pollution metrics), rendering direct merging infeasible; meanwhile, Tibet is excluded due to severe discontinuities in key environmental monitoring data. Second, representativeness. The agricultural sectors in HKMT constitute a negligible share of their respective GDPs and the national total; thus, their exclusion does not compromise the internal validity or the national-level applicability of the conclusions regarding the structural evolution of China's agricultural-ecological coordination. The indicators are primarily drawn from the CSMAR database, the *China Statistical Yearbook*, the *China Rural Statistical Yearbook*, the *China Statistical Yearbook on Environment and Resources*, the *Bulletin on the State of China's Ecological Environment*, as well as provincial (autonomous region and municipality) statistical yearbooks and statistical bulletins on national economic and social development. Rigorous data preprocessing was conducted to ensure reliability. We first examined the mechanism of missing data, which accounted for less than 1% of the total observations and exhibited a sporadic distribution. This pattern suggests a Missing at Random (MAR) mechanism rather than structural omission. On this basis, strictly distinguishing from simple mean imputation, we employed the Lagrange interpolation method to estimate missing values. This approach was selected for its superior ability to preserve the non-linear dynamic trends and continuity inherent in panel time-series data, thereby minimizing potential bias introduced by data gaps.

Building on the mechanism analysis in Section2, this study constructs an evaluation index system (Table 1) comprising two subsystems. The agricultural development subsystem (U_1) aims to characterize the comprehensive quality of agriculture from economic, social, and resource perspectives. The economic dimension captures industry scale and output efficiency (X_1 to X_9); the social dimension focuses on employment and rural livelihood (X_{10} to X_{14}); and the resource dimension reflects land utilization and green practices (X_{15} to X_{20}). It is worth noting that within the economic dimension, the "Disaster-stricken agricultural area" (X_9) is incorporated as an inverse indicator. Although post-disaster scenarios may theoretically trigger long-term ecological adaptation, within the specific observation period of this study, a higher disaster rate is primarily interpreted as a manifestation of the agricultural system's vulnerability to natural risks and acute production volatility, which negatively constrains the comprehensive development stability.

The ecological environment subsystem (U_2) reflects regional environmental carrying capacity and governance performance and is constructed strictly according to the Pressure-State-Response (PSR) framework to ensure theoretical consistency. Specifically, the "Environmental Pressure" (P) dimension captures the stress exerted by socioeconomic activities, such as resource consumption and pollutant emissions(Y_1 to Y_4).The "Environmental State" (S) dimension reflects the baseline quality of the ecosystem and service integrity (Y_5 to Y_8). Crucially, to resolve classification ambiguities in prior studies, the third dimension is strictly defined as "Environmental Response" (R) rather than the vague category of "Ecological Conservation." This dimension assesses the proactive governance inputs and remedial measures taken by human society to mitigate environmental degradation, such as fiscal expenditure on environmental protection and waste treatment rates (Y_9 to Y_{11}), thereby aligning the indicator system logically with the PSR theoretical framework. In the empirical analysis, all indicators are processed via scale-free normalization, and Confirmatory Factor Analysis (CFA) is applied to

230 extract composite development indices.

231 Table 1. Evaluation indicators for the development of agriculture and ecological environment

Subsystem	Criterion Layer	Sub-Criterion Layer	Order Parameter	Index Attribute
Agriculture U_1	economy	Total agricultural output value	X1	+
		Total crop output value	X2	+
		Agricultural added value	X3	+
		Grain production	X4	+
		Total mechanical power	X5	+
		Agricultural fiscal expenditure	X6	+
		Rural electricity consumption	X7	+
		Total export value of agricultural products	X8	+
		Disaster-stricken agricultural area	X9	-
	society	Number of people employed in agriculture	X10	+
		Rural residents' income	X11	+
		Per capita income of farmers	X12	+
		Per capita minimum social security expenditure in rural areas	X13	+
		Engel coefficient of rural households	X14	-
	resources	Cultivated land area	X15	+
		Crop sowing area	X16	+
		Effective irrigation area	X17	+
		Fertilizer usage	X18	-
		Agricultural film usage	X19	-
		Pesticide application rate	X20	-

Ecological Environment U_2	Environmental Pressure (P)	Energy Consumption per Unit of GDP	Y1	-
		Wastewater Discharge per Unit of GDP	Y2	-
		Solid Waste Discharge per Unit of GDP	Y3	-
		Air Pollutant Emissions per Unit of GDP	Y4	-
	Environmental State (S)	Forest Coverage Rate	Y5	+
		Density of National Nature Reserves	Y6	+
		Greening Coverage Rate of Built-up Areas	Y7	+
		Proportion of Days with Good Air Quality	Y8	+
	Ecological Response (E)	Share of Government Expenditure on Energy Conservation and Environmental Protection	Y9	+
		Centralized Treatment Rate of Urban Domestic Sewage	Y10	+
		Harmless Treatment Rate of Domestic Waste	Y11	+

4. Study Methods

To systematically portray the spatiotemporal evolution of the coupled and coordinated development between agricultural development and the ecological environment in China, this study builds an integrated methodological framework that links composite index construction –coupling coordination measurement – spatial differentiation diagnosis – dynamic evolution analysis – impact mechanism identification. Specifically, we employ confirmatory factor analysis (CFA), an optimized

coupling coordination degree (CCD) model, the Dagum Gini coefficient and its decomposition, Moran's I spatial autocorrelation index, kernel density estimation (KDE), a spatial Markov chain, and multiscale geographically weighted regression (MGWR).

4.1 Confirmatory factor analysis (CFA)

When constructing comprehensive indices for agricultural development and ecological environmental quality, many existing studies rely on objective weighting methods such as the entropy method. Although such methods are easy to implement and reduce subjective bias, they allocate weights purely according to the dispersion of indicators and thus tend to ignore the latent structure and theoretical relationships among indicators(Bao et al., 2020).

4.2 Optimized coupling coordination degree (CCD) model

After obtaining the agricultural development and ecological environment indices, we measure the interaction and harmony between the two subsystems using an optimized CCD model. Traditional CCD model has been widely applied, but recent work (Sj et al., 2021) points out several limitations in socio-economic applications, including weak sensitivity to structural differences and vulnerability to extreme values. Building on these insights, we improve the traditional CCD formulation to more faithfully represent the relationship between agricultural development and ecological environmental quality. this study has optimized the traditional CCD model as detailed below:

$$C_{\text{optimized}} = \sqrt{[1-\text{Var}(U)]\times\frac{1}{1+\exp\left(\frac{1}{n}\sum_{i=1}^{n}\ln\left(\frac{U_i}{M}\right)\right)}} \quad (1)$$

$$T = \sum_{i=1}^{n}\alpha_i \times U_i, \sum_{i=1}^{n}\alpha_i = 1 \quad (2)$$

$$D_{optimized} = \sqrt{C_{optimized}\times T} \quad (3)$$

Let U_i denote the comprehensive development index of a subsystem (agricultural development or ecological environment) for unit i, and $\mathrm{Var}(U)$ its variance. Let C denote the coupling degree, D the coordination degree, and T the comprehensive development index. Their specific expressions follow Eqs. (6) – (8). In this study, agriculture and the ecological environment constitute two subsystems ($n = 2$), and given their comparable importance for high-quality development and the "dual carbon" goals, we assign equal weights, i.e. $\alpha = \beta = 0.5$. Compared with the traditional CCD model, the optimized formulation has three main advantages: (1) By incorporating terms such as $|U_i - U_j|$, the model directly captures the deviation between subsystems, making the interpretation of "mismatch" between agricultural development and ecological environmental quality more intuitive; (2) In a coupled system, not only absolute levels but also the relative proportions and balance between subsystems matter. By introducing logarithmic means and exponential transformations, the optimized model focuses on the matching of subsystem structures while still reflecting their absolute development levels, which is consistent with the connotation of coordination; (3) Large regional disparities in either agricultural development or ecological environmental quality may generate extreme observations. The combined use of logarithmic and exponential terms improves the numerical distribution of the composite index, reducing the influence of outliers on $C$and D, and thereby enhancing the stability and reliability of the CCD results.

4.3 Dagum Gini coefficient and its decomposition

Considering the diverse economic development and ecological environment across China's regions, variations exist in the levels of coupled and coordinated development between these two systems. This study employs the Dagum Gini coefficient and decomposition method (Shi et al., 2020) to investigate these regional disparities and their temporal changes in the coupled and coordinated development between two systems within China. The formula as followed:

$$G = \frac{\sum_{j=1}^{k}\sum_{h=1}^{k}\sum_{i=1}^{n_j}\sum_{r=1}^{n_h}| x_{ji} - x_{hr} |}{2\gamma n^2} \quad (4)$$

In the equation, G represents the overall Gini coefficient, n signifies the total number of provinces in the sample, and k denotes the number of sections. n_j and n_h respectively indicate the number of provinces within the research sections where j and h are situated, while γ represents the average value of the coupling and coordination degree. Dagum decomposes the Gini coefficient into three components as $G=G_{nb}+G_w+G_t$, where G_w represents the distribution gap of the within-region CCD; G_{nb} reflects the distribution gap of the CCD between regions; and G_t denotes the impact of the cross-term of CCD between regions on the overall Gini coefficient G, known as super-density. If G_t, it indicates that the cross-term of the CCD between regions is absent. The specific equations are as follow from Eq.5 to Eq.9:

$$G_{jj} = \frac{\sum_{i=1}^{n_j}\sum_{r=1}^{n_j}\left|x_{ji} - x_{jr}\right|}{2n^2\gamma_j} \quad (5)$$

$$G_w = \sum_{j=1}^{k} G_{jj} p_j s_j \quad (6)$$

$$G_{jh} = \frac{\sum_{i=1}^{n_j}\sum_{r=1}^{n_j}\left|x_{ji} - x_{hr}\right|}{n_j n_h(\gamma_j + \gamma_h)} \quad (7)$$

$$G_{nb} = \sum_{j=2}^{k}\sum_{h=1}^{j=1} G_{jh}(p_j s_h + p_h s_j) D_{jh} \quad (8)$$

$$G_t = \sum_{j=2}^{k}\sum_{h=1}^{j=1} G_{jh}\left(p_j s_h + p_h s_j\right)(1 - D_{jh}) \quad (9)$$

4.4 Moran's I index

To investigate the spatial correlation properties and the temporal changes in spatial agglomeration of coupling and coordination between agriculture and ecological environment in China,

this study utilizes Moran's I index (Lee et al., 2017). The specific formula is as follows:

$$I = \frac{n}{\sum_{i=1}^{n}\sum_{j=1}^{n} w_{ij}} \frac{\sum_{i=1}^{n}\sum_{j=1}^{n} w_{ij}(x_i - \bar{x})(x_j - \bar{x})}{\sum_{i=1}^{n}(x_i - \bar{x})^2} \quad (10)$$

In this context, n signifies the total number of locations, whereas x_i and x_j represent the observed values at locations i and j, respectively.

4.5 Kernel density estimation (KDE)

Kernel density estimation (KDE) is a non-parametric estimation method, characterized by its independence from the chosen interval length, thereby exhibiting superior continuity(Kamalov, 2020). This study employs the Moran's I index to examine the spatial autocorrelation of the coupling and coordinated development process between agriculture and ecological environment. The kernel density function is as follows:

$$\hat{f}_h(x) = \frac{1}{n}\sum_{i=1}^{n} K_h(x - x_i) = \frac{1}{nh}\sum_{i=1}^{n} K\left(\frac{x - x_i}{h}\right) \quad (11)$$

Where, $K(x)$ represents the kernel function; n denotes the total number of samples, which in this study refers to the 30 provincial regions; h stands for the bandwidth of the density estimation.

4.6 Spatial Markov Chain analysis

To examine the spatial dynamics and evolutionary processes of coupled and coordinated development, this research employs the spatial Markov chain analysis method (Sharpe et al., 2021). The spatial Markov chain builds upon traditional Markov chains by incorporating "spatial lag" factors to condition the state transitions. Crucially, the specification of the spatial lag depends on the spatial weight matrix (W). In this study, to faithfully capture the mechanisms of cross-regional policy imitation and direct resource spillovers, we adopt the first-order Queen Contiguity Weight Matrix as the baseline specification. The elements of the matrix, w_{ij}, are defined as follows: $w_{ij} = 1$ if province i and

province j share a common boundary or vertex, and $w_{ij} = 0$ otherwise. The matrix is row-standardized to ensuring that the spatial lag represents the average coordination level of the neighborhood. The calculation of the spatial lag is expressed as:

$$Lag_i = \sum_{j=1}^{n} w_{ij} Y_j \tag{12}$$

Where Y_j represents the CCD value of neighboring province j. Based on the calculated Lag_i, the spatial neighborhood conditions are discretized into different classes (e.g., Low, Medium, High). The transition probabilities are then estimated conditional on these spatial lag classes.

The conditional transition probability matrix is defined as $P_{ij}(k)$, representing the probability that a region transitions from state *i* to *j* under neighborhood condition *k*, and $n_i(k)$ is the total count of regions in state *i* with neighborhood *k*:

$$P_{ij}(k) = \frac{n_{ij}(k)}{n_i(k)} \tag{13}$$

where $n_{ij}(k)$ denotes the number of regions transitioning from state *i* to *j* under neighborhood condition *k*, and $n_i(k)$ is the total count of regions in state *i* with neighborhood *k*.

4.7 Multiscale Geographically Weighted Regression

MGWR (Hu et al., 2022) represents a sophisticated spatial analytical approach capable of identifying distinct spatial scales at which various explanatory variables affect regional outcomes, thereby accurately capturing spatial non-stationarity in their impacts. The model specification is constructed as:

$$CCD_i = \beta_0 + \beta_1 AES_i + \beta_2 EEL_i + \beta_3 REDL_i + \beta_4 IIL_i + \beta_5 EEQ_i + \varsigma_i \tag{14}$$

The explanatory variables are selected based on the "Driver-Pressure-State" mechanism: Agricultural Economic Scale (AES) is proxied by per capita gross output of agriculture and related sectors; Ecological Environment Level (EEL) by the development index of regional ecological construction

and environmental governance; Regional Economic Development Level (REDL) by per capita GDP; Infrastructure Investment Level (IIL) by road network density; and Ecological Environmental Quality (EEQ) by forest coverage rate. Critically, variables such as agricultural fiscal subsidies and carbon emission intensity are deliberately excluded to avoid endogeneity and multicollinearity, as these indicators are already constitutive elements of the dependent variable (CCD) calculation. In the estimation, the corrected Akaike Information Criterion (AICc) is utilized for optimal bandwidth selection via a back-fitting algorithm, ensuring the best balance between model fit and complexity.

5. Results and Discussion

5.1 Time evolution analysis of CCD

Building on the optimized CCD model, this study measures the CCD between agricultural development and the ecological environment for 30 Chinese provinces over 2013–2022; the results are reported in Table 3. Following Liu's classification framework (Table 2), the CCD is divided into six levels, severe discoordination, slight discoordination, near discoordination, primary coordination, intermediate coordination, and advanced coordination, with specific threshold criteria shown in Table 2. To intuitively illustrate the evolution of the coupling–coordination level, descriptive statistical plots are provided in Figure 2. As shown in Figure 2, the agriculture–ecological environment CCD for the 30 provinces exhibits a steadily increasing trend during 2013–2022 and, on average, has reached the stage of primary coordination. This indicates that the positive linkage and synergistic effects between agricultural development and environmental protection have been continuously strengthened, and that the system as a whole is gradually shifting from "discoordination–bare coordination" toward "coordinated development." It is noteworthy that the CCD level experienced a temporary decline in 2020 under the shock of the COVID-19 pandemic, which is consistent with the findings of Wang et al.(Wang et al., 2022) and Cao et al. (Cao et al., 2020) regarding the substantial negative impacts of

the pandemic on agriculture, thereby disturbing the coevolution of the agricultural and ecological systems. In addition, the presence of outliers in each year in Figure 2 reflects pronounced interregional disparities in the agriculture–environment CCD, suggesting that the problem of unbalanced regional development remains salient.

Table 2. State level of CCD

CCD value	State level	CCD value	State level
(0.0, 0.2]	Serious disorders (State 1)	(0.4, 0.6]	Primary coordination (State 4)
(0.2, 0.3]	Slight disorders (State 2)	(0.6, 0.8]	Intermediate coordination (State 5)
(0.3, 0.4]	Barely coordination (State 3)	(0.8, 0.10]	Senior coordination (State 6)

Table 3. The results of CCD in 30 provincial regions from 2013 to 2022

Province	2013	2014	2015	2016	2017	2018	2019	2020	2021	2022
Beijing	0.454	0.481	0.491	0.508	0.522	0.537	0.569	0.575	0.579	0.595
Tianjin	0.433	0.446	0.449	0.462	0.467	0.475	0.514	0.517	0.547	0.564
Hebei	0.428	0.443	0.450	0.467	0.477	0.478	0.494	0.484	0.506	0.517
Shanxi	0.386	0.398	0.417	0.427	0.437	0.446	0.463	0.453	0.475	0.487
Nei Menggu	0.411	0.419	0.433	0.443	0.448	0.460	0.478	0.464	0.480	0.495
Liaoning	0.397	0.416	0.434	0.444	0.456	0.463	0.482	0.470	0.491	0.501
Jilin	0.412	0.417	0.429	0.439	0.446	0.475	0.474	0.464	0.482	0.497
Hei Longjiang	0.401	0.417	0.445	0.464	0.470	0.485	0.506	0.496	0.518	0.529
Shanghai	0.413	0.417	0.433	0.456	0.462	0.488	0.529	0.514	0.517	0.539
Jiangsu	0.399	0.412	0.425	0.440	0.447	0.461	0.477	0.476	0.491	0.513
Zhejiang	0.401	0.419	0.427	0.447	0.455	0.468	0.488	0.484	0.497	0.511
Anhui	0.376	0.389	0.409	0.423	0.434	0.453	0.469	0.459	0.487	0.493
Fujian	0.385	0.401	0.422	0.439	0.447	0.459	0.479	0.469	0.477	0.493
Jiangxi	0.371	0.384	0.397	0.410	0.418	0.433	0.449	0.442	0.459	0.469
Shandong	0.410	0.428	0.432	0.443	0.450	0.462	0.484	0.475	0.485	0.490
Henan	0.385	0.396	0.408	0.425	0.429	0.442	0.461	0.454	0.463	0.476
Hubei	0.366	0.383	0.400	0.415	0.412	0.422	0.440	0.427	0.445	0.457

Hunan	0.376	0.387	0.407	0.415	0.421	0.431	0.447	0.440	0.446	0.457
Guangdong	0.352	0.365	0.383	0.400	0.409	0.421	0.443	0.432	0.451	0.465
Guangxi	0.351	0.366	0.386	0.400	0.415	0.434	0.456	0.446	0.455	0.468
Hainan	0.362	0.375	0.392	0.409	0.415	0.435	0.448	0.435	0.442	0.454
Chongqing	0.329	0.347	0.369	0.390	0.396	0.411	0.430	0.433	0.457	0.473
Sichuan	0.355	0.365	0.376	0.391	0.396	0.406	0.418	0.414	0.418	0.431
Guizhou	0.328	0.335	0.360	0.375	0.387	0.396	0.412	0.406	0.419	0.423
Yunnan	0.342	0.352	0.363	0.376	0.386	0.394	0.406	0.399	0.407	0.411
Shaanxi	0.332	0.345	0.361	0.374	0.384	0.392	0.407	0.400	0.407	0.423
Gansu	0.307	0.323	0.340	0.358	0.366	0.378	0.395	0.390	0.402	0.414
Qinghai	0.317	0.325	0.340	0.353	0.357	0.362	0.378	0.373	0.391	0.408
Ningxia	0.297	0.313	0.343	0.352	0.360	0.368	0.386	0.402	0.440	0.451
Xinjiang	0.305	0.320	0.338	0.343	0.354	0.361	0.379	0.366	0.388	0.394

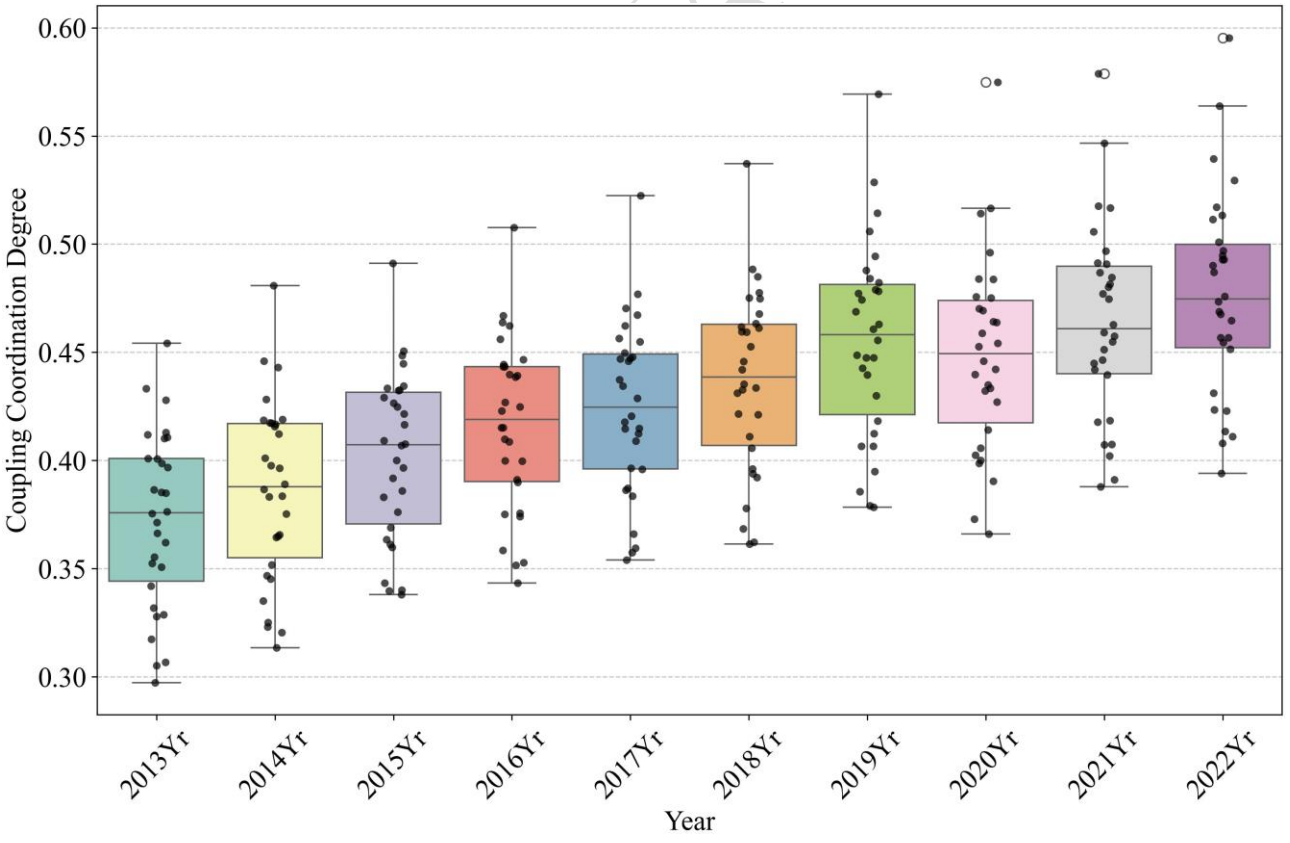

Figure 2. Descriptive statistical results of CCD from 2013 to 2022

Based on Figure 3, the spatial distribution of coupling coordination between agriculture and the

ecological environment exhibits a clear “high in the east, low in the west” pattern throughout the study period. Most provinces show a gradual increase in their CCD values, with eastern and coastal regions demonstrating notably higher levels of coordination between agricultural development and environmental protection—consistent with the overall upward trend depicted in Figure3. In contrast, the western region maintains relatively low CCD values, indicating that pronounced regional development imbalances persist.

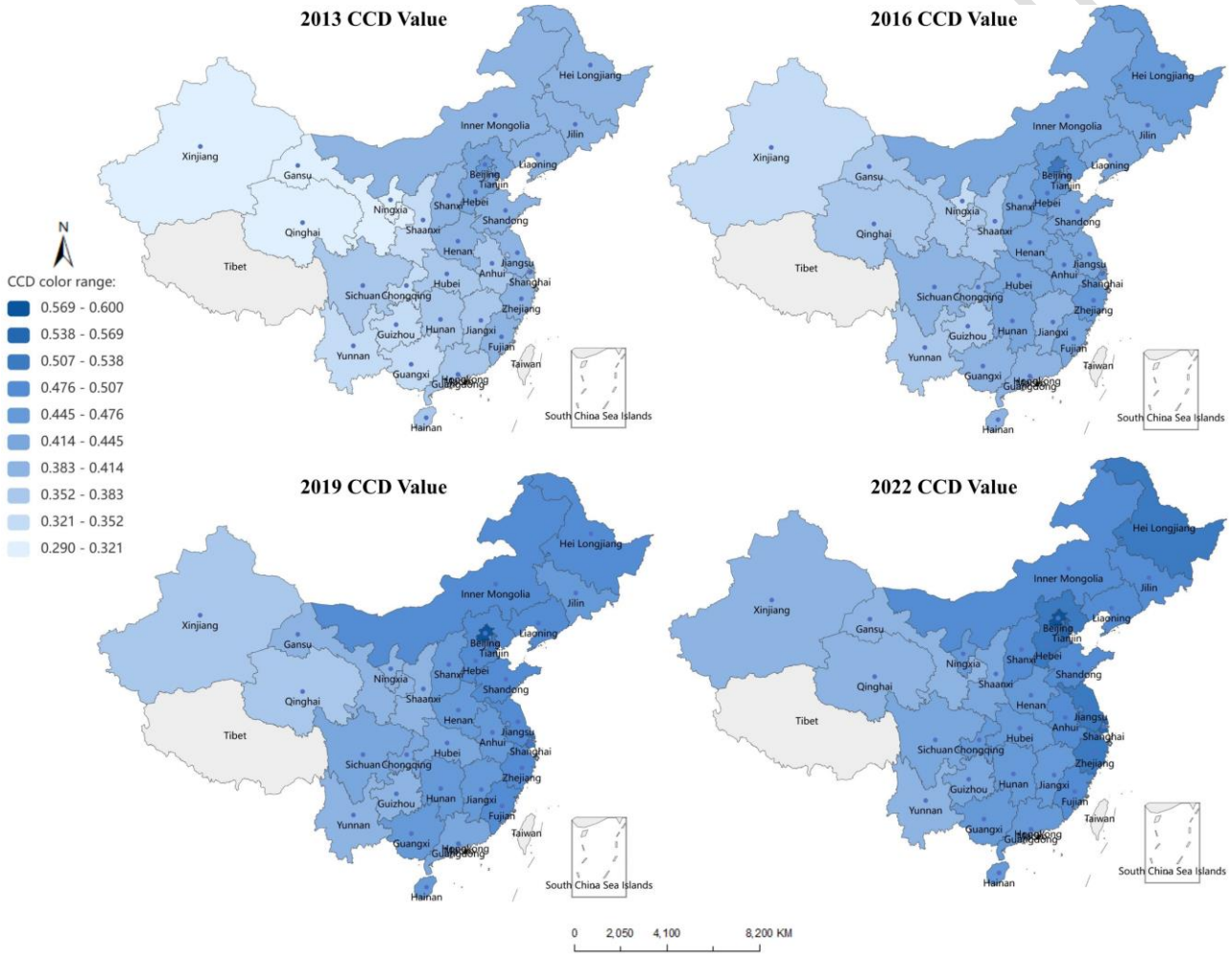

Figure 3. Spatial distribution changes in the CCD for 30 provinces in China

Building on the overall evolutionary analysis, this study further employs the Dagum Gini coefficient and its decomposition to systematically examine the respective contributions of within region and between region disparities in the coupling coordination of agriculture and the ecological environment, thereby identifying the main sources and dynamic evolution of regional differences.

The computed Dagum Gini coefficients are reported in Table 4, and their temporal trends are visualized in Figure 4. As shown in Figure 4(a), the overall Gini coefficient for the agriculture–ecological environment coupling coordination degree exhibits a gradual downward trend during 2013–2022, indicating a general convergence of regional disparities. This pattern is closely related to the implementation of strategies such as rural revitalization and to the efforts of central and western regions to leverage their resource endowments to promote green agricultural development and ecological governance. Through the development of specialty agriculture and ecological construction, the central and western regions have gradually narrowed their gap with the east. Figure 4(b) shows that between region disparities remain the dominant source of the overall Gini coefficient, with their contribution consistently exceeding 70 percent. This suggests that differences in agricultural development foundations, ecological carrying capacity, and green transition capabilities across regions are still the core determinants of heterogeneity in the agriculture–ecological environment coupling coordination level. Figure 4(c) indicates that within region disparities are largest in the eastern region, primarily because the coordination level of agriculture and the ecological environment in coastal, economically advanced provinces is markedly higher than that in some inland provinces. The central region ranks second, while the western and northeastern regions display relatively small internal differences, which is related to their high dependence on natural resources and the strong homogeneity of their industrial structures. Figure 4(d) further reveals that the main component of between region disparity arises from the gap between the eastern and western regions, followed by the differences between the east and the central and northeastern regions. This pattern reflects not only the comprehensive advantages of the eastern region in agricultural modernization and environmental governance, but also the relative lag in infrastructure and green development capacity in the central and western regions. Overall, regional disparities in the agriculture–ecological

environment coupling coordination degree are mainly driven by unbalanced development between the eastern region and other regions, as well as internal imbalances within the east.

Tabe 4. Dagum Gini coefficient and contribution rate results

Year	Gini coefficient				Contribution rate （%）		
	Overall	intra-regional	Inter-regional	hyper-variable	Intra-regional (%)	Inter-regional (%)	hyper-variable density (%)
2013	0.061	0.011	0.044	0.006	18.24	72.25	9.51
2014	0.060	0.011	0.044	0.005	17.76	73.79	8.45
2015	0.054	0.009	0.040	0.004	17.31	74.75	7.94
2016	0.053	0.009	0.040	0.004	17.42	75.21	7.37
2017	0.052	0.009	0.039	0.004	17.97	74.99	7.04
2018	0.053	0.010	0.040	0.003	17.90	76.16	5.95
2019	0.055	0.010	0.041	0.004	18.53	74.76	6.71
2020	0.055	0.011	0.041	0.004	19.24	74.09	6.67
2021	0.054	0.011	0.038	0.005	19.89	71.68	8.42
2022	0.054	0.011	0.039	0.004	19.96	72.00	8.04

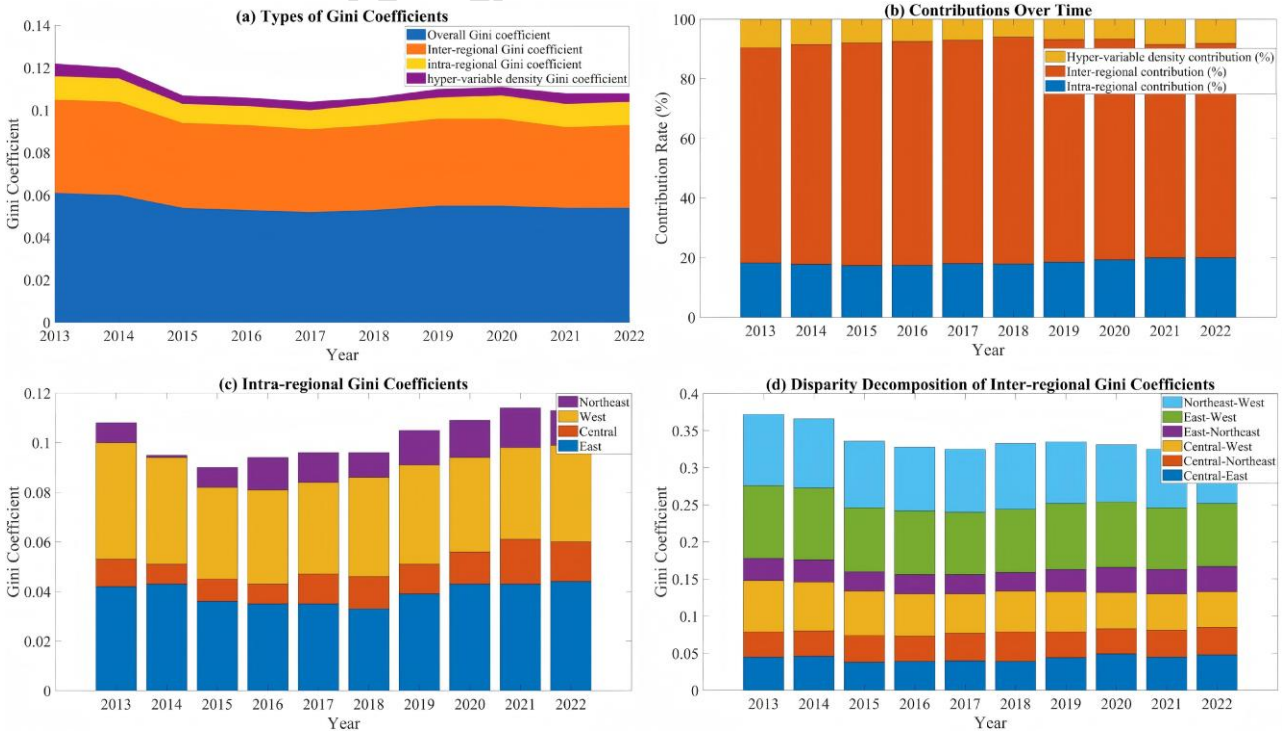

Figure 4. Temporal analysis of Dagum Gini Coefficients and their decomposition by regions (2013-2022)

To further reveal the dynamic distribution characteristics and long-term evolutionary patterns of coupling coordination levels across regions, this study employs Kernel Density Estimation (KDE) to analyze the CCD in the eastern, central, western, and northeastern regions. This approach is used to determine whether each region exhibits a tendency toward convergence, divergence, or polarization, and, on this basis, to assess the potential and constraints of coordinated development in different regions. Figure 5 illustrates the dynamic evolution of the distribution of coupling coordination degrees across 30 provinces from 2013 to 2022. The evolution of the kernel density curves reveals three critical stylized facts regarding the spatial distribution pattern. First, regarding the location, the center of the distribution curve demonstrates a consistent "rightward shift," indicating that the average level of agricultural-ecological coordination in China is steadily improving. Second, concerning the distribution shape (Kurtosis and Skewness), the curve exhibits a clear trajectory of "peak height decreasing and width expanding," accompanied by a significant "right-trailing" phenomenon. Economically, this implies that while the overall coordination is improving, the absolute disparity between regions is widening. The "platykurtic" transformation suggests that the convergence speed of lagging regions is slower than the breakthrough speed of leading regions, resulting in a dispersed spatial pattern. Third, regarding polarization trends (Multimodality), the curve evolves from a standard "single-peak" to a "weak double-peak" or "multi-peak" pattern in the later years. This emergence of multimodality signals a potential risk of "club convergence" and spatial stratification. It suggests that the coupled development is transitioning from a uniform distribution to a polarized structure, where distinct "high-level clubs" (likely in the coastal east) and "low-level traps" (in the western inland) are solidifying. This validates the "Matthew Effect" hypothesis proposed in Section 2, highlighting the urgent need for differentiated regional policies to break this spatial solidification.

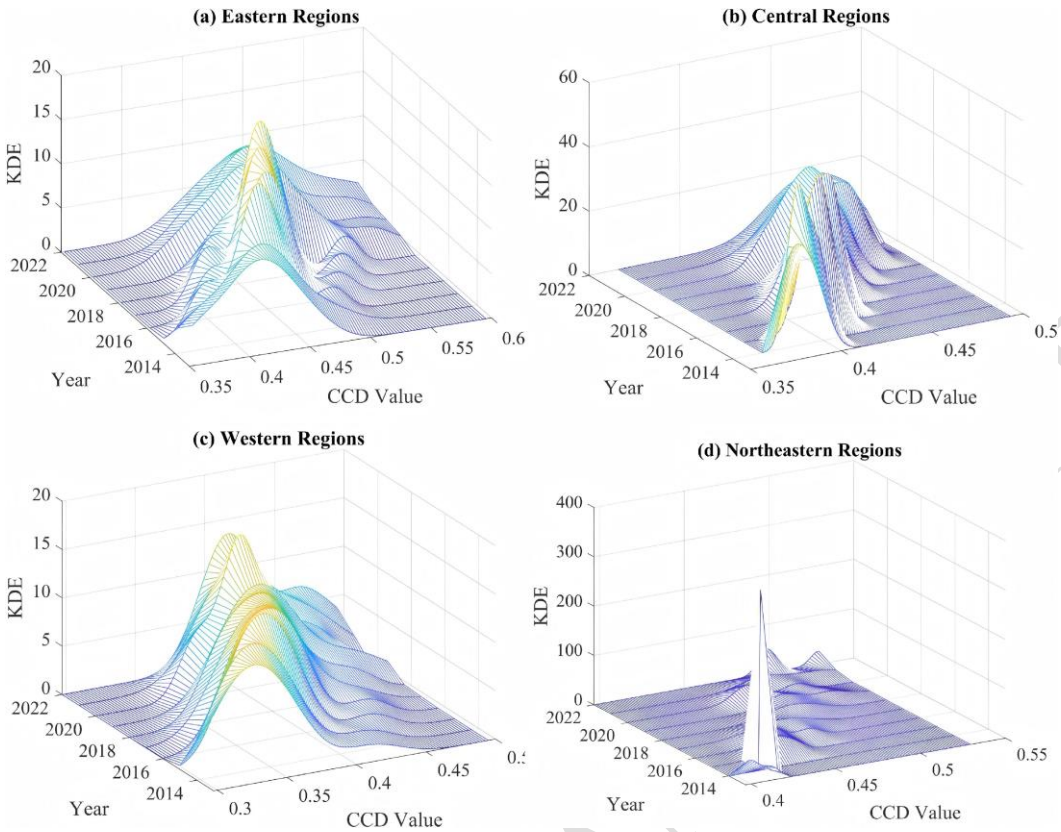

Figure5. Kernel Density Distribution Curve of CCD Level from 2013 to 2022

5.2 Spatial evolution analysis

To further reveal the spatial agglomeration characteristics and evolutionary patterns of the coupling coordination between agricultural development and the ecological environment, this study first applies a global spatial autocorrelation approach, with the results reported in Table 5. As shown in Table 5, the Moran's I index for the coupling coordination degree of agriculture and the ecological environment at the national level remains between approximately 0.60 and 0.68 during 2013–2022, and the corresponding Z-values are all significantly positive at the 1% significance level. This indicates that, at the provincial scale, the coupling coordination degree of agriculture and the ecological environment consistently exhibits significant positive spatial correlation and a stable, pronounced spatial clustering pattern. Although the annual Moran's I value fluctuate slightly, the overall level of spatial agglomeration remains high, suggesting strong consistency and linkage among neighboring regions in terms of their agriculture–ecological environment coordination level.

Table 5. Spatial correlation of coupled and coordinated development level

Year	Moran's I	Z-Score	P-Value
2013	0.667220	5.720445	0.000
2014	0.679810	5.830607	0.000
2015	0.671588	5.755226	0.000
2016	0.623252	5.385146	0.000
2017	0.621854	5.487798	0.000
2018	0.602511	5.172523	0.000
2019	0.604820	5.308829	0.000
2020	0.601891	5.351504	0.000
2021	0.647375	5.688023	0.000
2022	0.629823	5.461400	0.000

To further identify the spatial agglomeration patterns and their specific locations, the Local Moran's I scatter plots and LISA cluster maps (Figure 6) were generated, revealing distinct spatial clubs driven by divergent economic forces. The High-High (H-H) agglomeration is stably concentrated in the eastern coastal regions, primarily covering Jiangsu, Zhejiang, Shanghai, Shandong, and Fujian. The formation of this "High-High" club is fundamentally driven by positive inter-regional spillover effects; these regions possess advanced agricultural technologies and stringent environmental regulations, where the mechanism of "learning by doing" and cross-regional policy coordination allows green innovation to rapidly diffuse to neighbors, thereby creating a synergistic highland of high-quality coordinated development. In stark contrast, the Low-Low (L-L) agglomeration area is mainly distributed in the western and northeastern regions, including Gansu, Ningxia, Xinjiang, Inner Mongolia, and Jilin. The persistence of this "Low-Low" trap is attributable to the dual constraints of natural endowments and economic structure: on the one hand, ecological fragility (such as water scarcity in the Northwest) limits the carrying capacity for high-intensity agriculture; on the other hand, the "siphon effect" from eastern regions leads to the outflow of capital

and talent, leaving these areas locked in a path dependence of extensive, resource-consuming agricultural production. Furthermore, scattered Low-High (L-H) areas (e.g., Anhui and Jiangxi) serve as transitional zones that—due to administrative barriers or insufficient absorptive capacity—have not yet fully absorbed the spillover dividends from developed neighbors, reflecting a significant "core-periphery" gradient structure in the spatial layout.

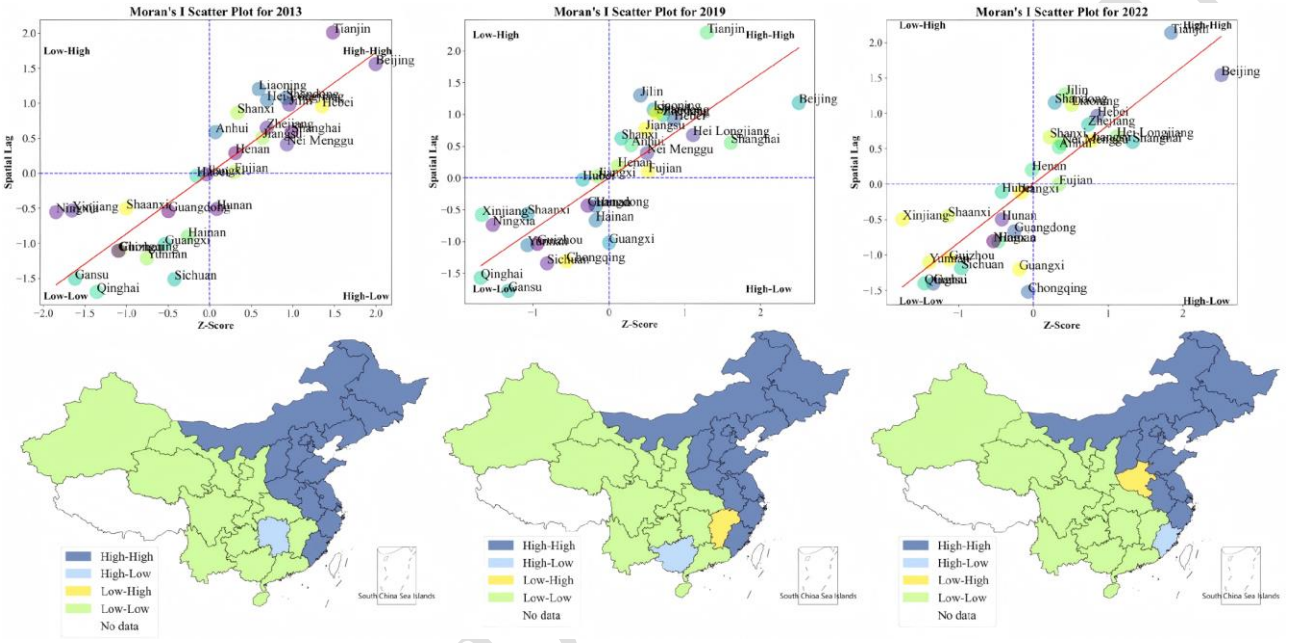

Figure6. Moran Scatter Plot for 30 provincial regions

Building on the identification of overall spatial correlation and local clustering patterns, this study further conducts a hot spot and cold spot analysis to characterize the spatiotemporal evolution of high-value and low-value agglomeration areas. The results are presented in Figure 7. As shown in Figure 7, hot spots of the agriculture–ecological environment coupling coordination degree are mainly concentrated in the eastern coastal region and several central provinces, and they persist as significant hot spots across all years, with gradually increasing hotspot intensity (confidence levels). This indicates that the synergistic effects of green agricultural development and ecological governance in these areas have been continuously strengthened. Cold spots are primarily located in the western region. Although the spatial extent of cold spots has narrowed during 2014–2022, the core cold spot areas have remained in a state of low coordination over a long period. This pattern

suggests that some western provinces still face pronounced weaknesses in terms of the foundations for agricultural modernization, environmental carrying capacity, and green development capability. Overall, the spatial distribution of the agriculture–ecological environment coupling coordination degree exhibits a “strong east, weak west” pattern. Regional disparities have somewhat converged, but they have not yet been fundamentally eliminated.

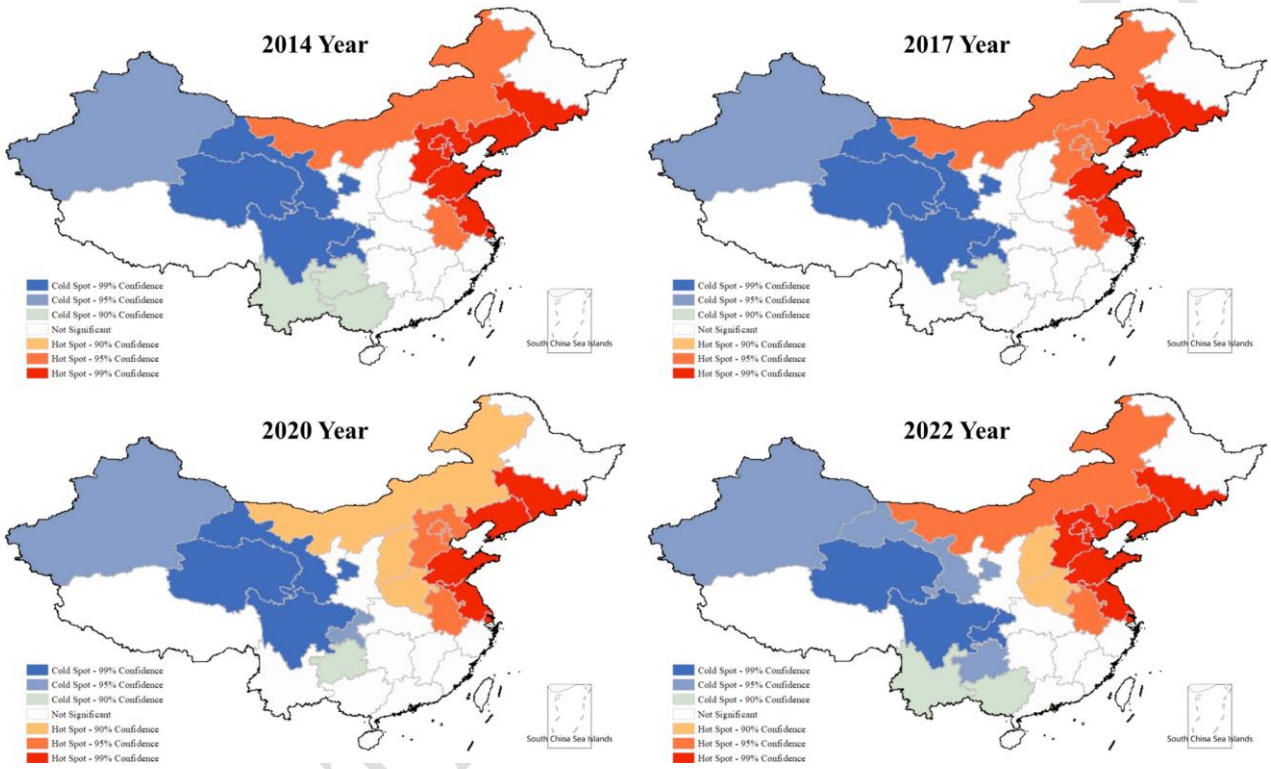

Figure7. Cold and hot spot clustering analysis

To further analyze the dynamic transition characteristics of different coupling coordination states under spatial influence after identifying spatial patterns and hot–cold spot evolution, this study introduces a spatial Markov chain. The corresponding transition probability matrix is shown in Figure8. As indicated in Figure 8, the coupling coordination level between agriculture and the ecological environment exhibits pronounced path dependence. The probabilities along the main diagonal are generally high, suggesting strong state persistence at the original coordination level across regions. The stability of high-level coordination states is particularly notable, implying that these regions have already developed relatively mature modes of coordinated agriculture–

environment development and possess strong capacities for resource agglomeration and policy support. Low-level coordination states also display a high probability of self-locking, and the probability of leaping directly from a low to a high coordination state is close to zero, which reflects a clear "Matthew effect." At the same time, the matrix results reveal spatial spillover effects. Some low-level regions have relatively high probabilities of transitioning to lower-middle or medium coordination states, indicating that neighboring high-level regions exert a certain radiative and driving effect. However, this effect is not sufficient to bridge overall development gaps in the short term. Overall, the spatial evolution of agriculture–ecological environment coupling coordination in China can be characterized as "high-level consolidation, low-level lock-in, and limited neighborhood spillover." For low-coordination regions, achieving leapfrog improvements still depends on stronger policy interventions, more effective resource integration, and enhanced mechanisms of regional collaborative governance.

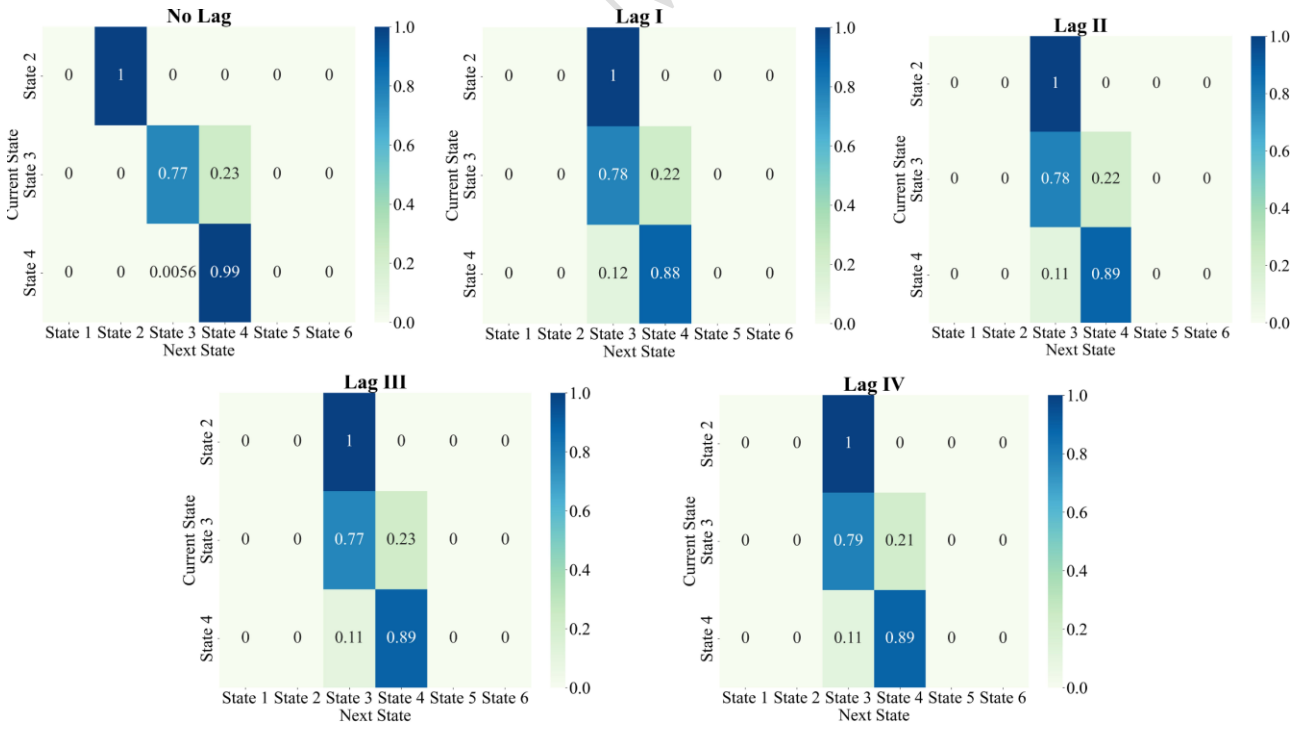

Figure8. The state transition probability matrix for a lag of 4 periods

Further investigation into the role of administrative divisions reveals significant heterogeneity in the coupling coordination process. As evidenced in Table 3, Municipalities directly under the

Central Government (e.g., Beijing, Shanghai) exhibit consistently higher CCD values, benefiting from concentrated policy resources and advanced governance capabilities. Conversely, Autonomous Regions (e.g., Xinjiang, Ningxia), often constrained by ecological fragility and heavy reliance on traditional agriculture, generally lag behind in coordination levels. This distinction underscores that administrative status, entailing different fiscal autonomies and resource endowments, serves as a critical institutional factor shaping the spatial evolution of the coupled system alongside geographical location.

5.3 Spatial Non-stationarity Analysis of Influencing Factors on the Coupled and Coordinated Development

To uncover the distinct spatial scales and heterogeneous impacts of driving factors, this study employed the MGWR model. Prior to the specific analysis, we validated the MGWR model's superiority through a comparative diagnostic. The results confirm that MGWR provides a significantly better fit, evidenced by a markedly lower AICc value (-68.42) and a higher adjusted. R^2 compared to the traditional GWR model. This statistical evidence verifies that allowing for multi-scale bandwidths effectively captures complex spatial heterogeneity. Based on the validated model, the estimation results in Table 6 and Figure 9 reveal distinct action scales rooted in different economic mechanisms. Variables such as Infrastructure Investment (IIL) and Regional Economic Development (REDL) exhibit narrow bandwidths (57 and 106, respectively). This strong spatial non-stationarity indicates that the spillover effects of physical capital are constrained by administrative segmentation and local protectionism, behaving as "local public goods" with rapid distance-decay. In contrast, Ecological Environmental Quality (EEQ) demonstrates a broad bandwidth (129), operating at a near-global scale, which reflects the non-excludability and cross-regional fluidity of ecosystem services (e.g., air purification) that transcend provincial borders.

548 Table 6. MGWR Model Estimation Results

Panel A: Model Diagnostic Comparison			
Model	**AICc**	**Adjusted R^2**	**Residual Sum of Squares**
MGWR	-68.42	0.895	4.21
GWR	-54.15	0.812	5.67
OLS	-32.1	0.654	12.89

Panel B: MGWR Variable Estimation Results						
Variables	**Global Parameter**	**Min Local**	**Max Local**	**Mean Local**	**Bandwidth**	**Spatial Non-stationarity**
Agricultural Economic Scale (AES)	0.342**	0.113	0.612**	0.356	82	Moderate
Ecological Environment Level (EEL)	0.519***	0.223*	0.817***	0.527	64	High
Regional Economic Dev. (REDL)	0.295**	0.104	0.487**	0.301	106	Moderate
Infrastructure Investment (IIL)	0.417***	0.210*	0.672***	0.425	57	High
Ecological Env. Quality (EEQ)	0.238*	0.073	0.401**	0.242	129	Low
Constant (Intercept)	0.112	-0.054	0.321	0.156	45	-

549 Note: "**" indicates significance at the 1% level, "*" at the 5% level, and "*" at the 10% level.

550

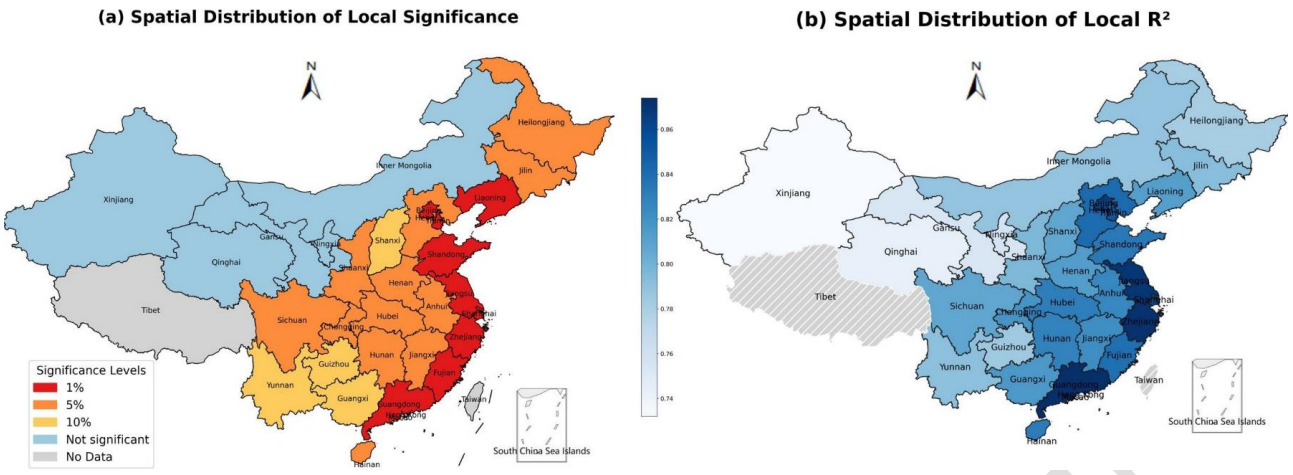

Figure 9. Spatial distribution of local significance and local R^2

Furthermore, the local regression coefficients presented in Table 7 and Figure 10 highlight a clear "East-West" gradient driven by varying marginal productivities. Factors representing development foundations—specifically Agricultural Economic Scale (AES) and IIL—exert significantly stronger positive effects in eastern coastal provinces than in the west. Economically, this suggests that the Eastern region has achieved "Agglomeration Economies," where high factor density reduces green technology transaction costs and generates increasing returns to scale. Conversely, in western provinces, the coefficients for these drivers are lower. This is attributable to the "Binding Constraint" of ecological fragility: in these regions, purely increasing economic inputs yields diminishing marginal returns due to the rigid limits of environmental carrying capacity. Notably, Ecological Environment Level (EEL) and Ecological Environmental Quality (EEQ) maintain robust influence across the central and western regions. This underscores that strictly preserving natural capital and enhancing ecological governance are the fundamental preconditions for avoiding the "poverty-environment trap" in resource-dependent areas.

Table 7. Local Estimation Results of MGWR for Coupled and Coordinated Development between Agriculture and Environment at the Provincial Level in China

Province	AES	EEL	REDL	IIL	EEQ
Beijing	0.452**	0.817***	0.487***	0.672***	0.245*
Tianjin	0.440**	0.783***	0.462***	0.647***	0.239*
Hebei	0.412**	0.721***	0.455***	0.621***	0.234*
Shanxi	0.376*	0.612**	0.372**	0.558**	0.222*

Nei Menggu	0.322*	0.544**	0.361**	0.487**	0.311**
Liaoning	0.364*	0.650***	0.387**	0.532***	0.260*
Jilin	0.310*	0.511**	0.338**	0.468**	0.325**
Hei Longjiang	0.299*	0.523**	0.326**	0.455**	0.320**
Shanghai	0.431**	0.789***	0.473***	0.665***	0.238*
Jiangsu	0.478**	0.802***	0.481***	0.673***	0.278**
Zhejiang	0.467**	0.799***	0.472***	0.669***	0.401***
Anhui	0.390*	0.672***	0.412**	0.598***	0.252*
Fujian	0.418**	0.738***	0.435***	0.621***	0.398***
Jiangxi	0.357*	0.642***	0.396**	0.578***	0.315**
Shandong	0.399**	0.688***	0.423**	0.615***	0.265*
Henan	0.367*	0.633**	0.392**	0.587**	0.249*
Hubei	0.403**	0.667***	0.417**	0.609***	0.286**
Hunan	0.368*	0.651***	0.398**	0.593***	0.321**
Guangdong	0.489***	0.811***	0.481***	0.671***	0.332**
Guangxi	0.346*	0.621***	0.383**	0.572***	0.356**
Hainan	0.362*	0.688***	0.397**	0.599***	0.378**
Chongqing	0.348*	0.654***	0.385**	0.575***	0.342**
Sichuan	0.330*	0.611***	0.372**	0.552**	0.358**
Guizhou	0.278*	0.534**	0.328**	0.468**	0.366**
Yunnan	0.291*	0.522**	0.339**	0.482**	0.401***
Shaanxi	0.320*	0.558**	0.351**	0.502**	0.288**
Gansu	0.246	0.326*	0.273*	0.321*	0.21
Qinghai	0.219	0.287*	0.256*	0.298*	0.202
Ningxia	0.231	0.313*	0.268*	0.309*	0.222*
Xinjiang	0.211	0.223*	0.239*	0.210*	0.218*

570

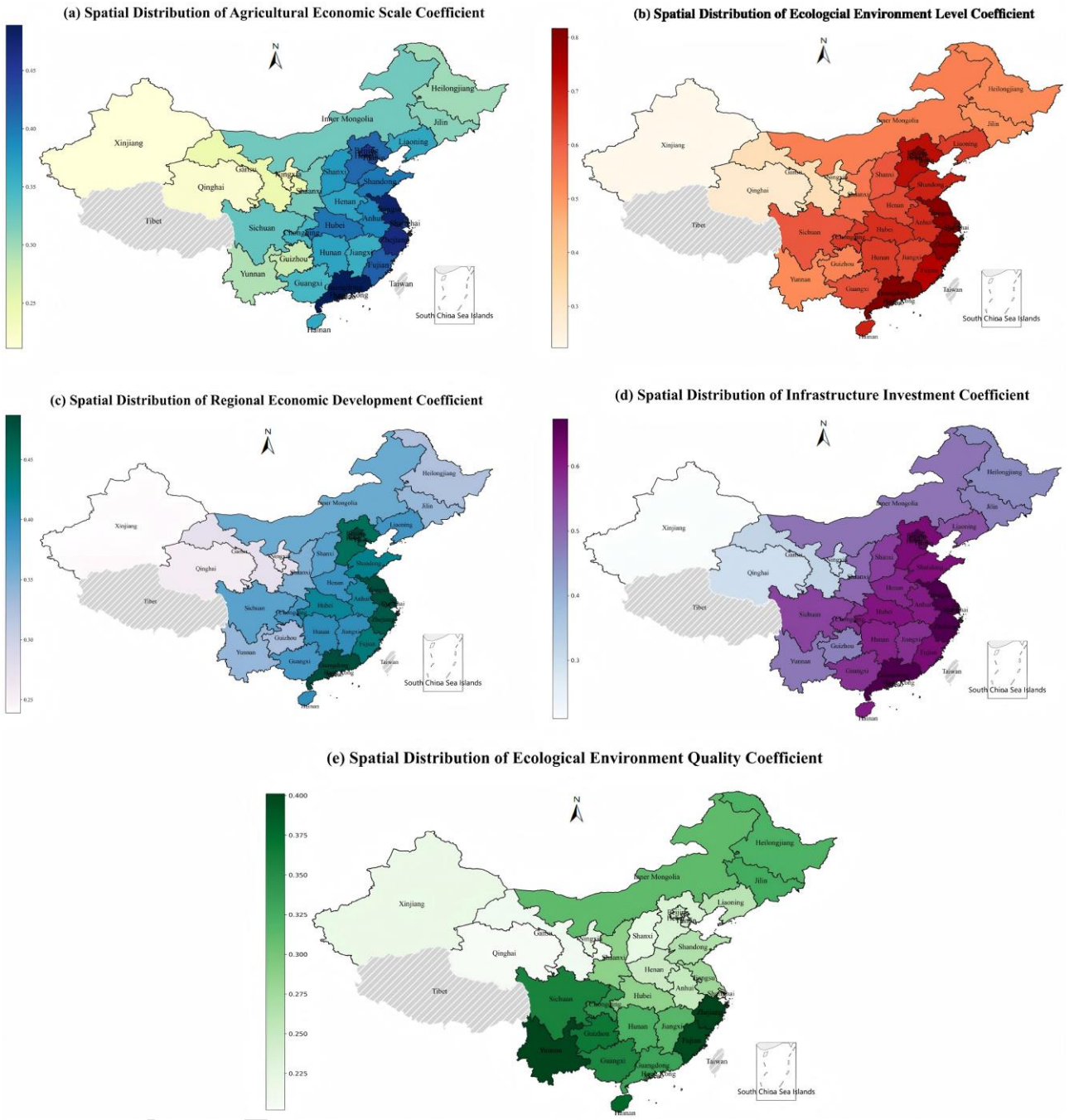

Figure10. Spatial distribution of local regression coefficients for each factor

5.4 Robustness Check and Sensitivity Analysis

To ensure the reliability of the empirical findings and validate the methodological advantage of the optimized CCD model, this study conducts a systematic robustness check involving model comparison and parameter sensitivity analysis. As illustrated in Figure 11, it contrasts the probability density distributions of the optimized CCD model against the traditional geometric mean model. As observed, the traditional model (blue dashed line) exhibits a pronounced leptokurtic pattern,

clustering values in a narrow range which limits the identification of regional differences. In contrast, the optimized model (red solid line) displays a platykurtic distribution with a broader span. This transformation yields two critical advantages: it significantly enhances the distinguishability of subtle structural disparities often masked by the traditional approach, and mitigates the underestimation bias inherent in geometric means. The consistent performance across all four regions confirms the optimized model's robustness in capturing spatial heterogeneity.

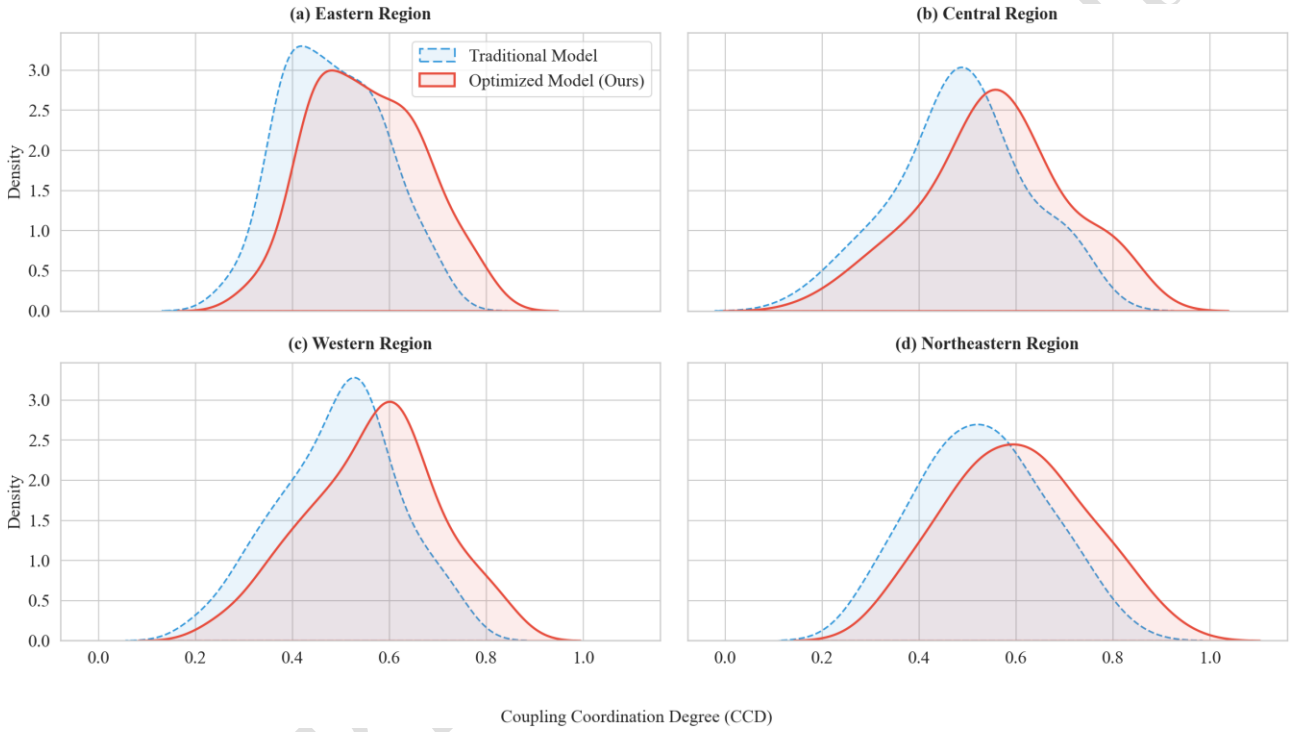

Figure 11. Comparison of kernel density estimates between the traditional and optimized CCD models across four major regions.

Having established the structural superiority, it is imperative to further verify that the results are robust outcomes of system dynamics rather than artifacts of subjective weight assignments. Figure 12 depicts the temporal evolution of CCD under varying weight specifications. The trajectories for Agriculture-Priority ($\alpha = 0.6$) and Ecology-Priority ($\alpha = 0.4$) scenarios are tightly confined within a narrow "robustness envelope" around the Baseline. The zoomed inset corroborates that the secular upward trend remains structurally invariant.

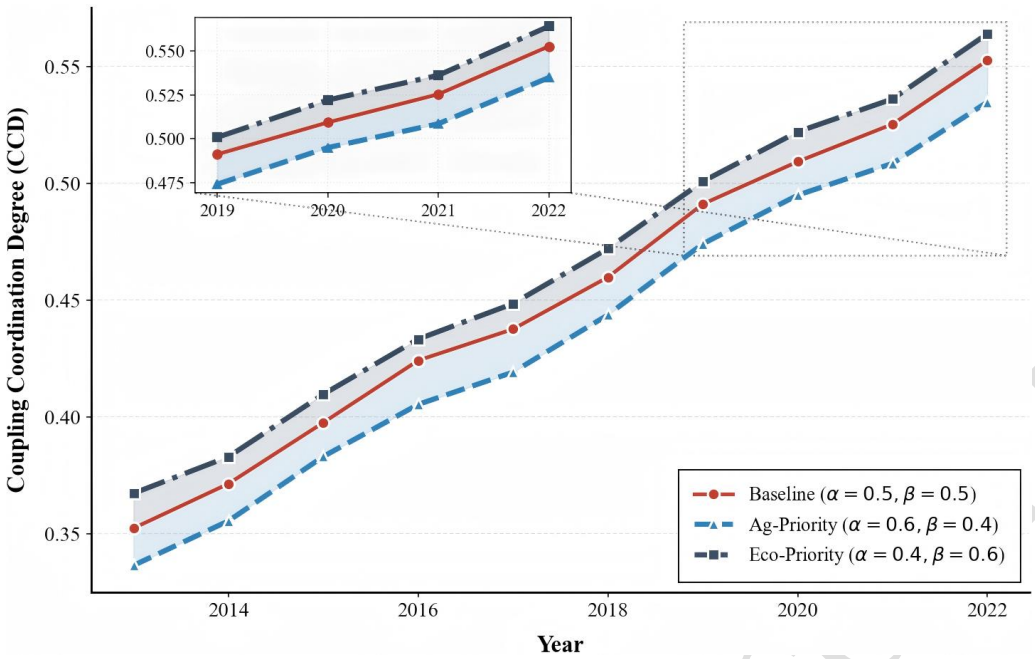

Figure 12. Temporal evolution and sensitivity analysis of the CCD under parameter uncertainty

Furthermore, we conducted a rank invariance analysis to assess the stability of relative positioning (Figure 13). The scatter points are densely clustered around the 45° diagonal line, with a Pearson correlation coefficient of 0.985 ($p < 0.001$). This confirms that the identification of leading and lagging regions is not driven by parameter subjectivity, thereby substantiating the validity of our conclusions.

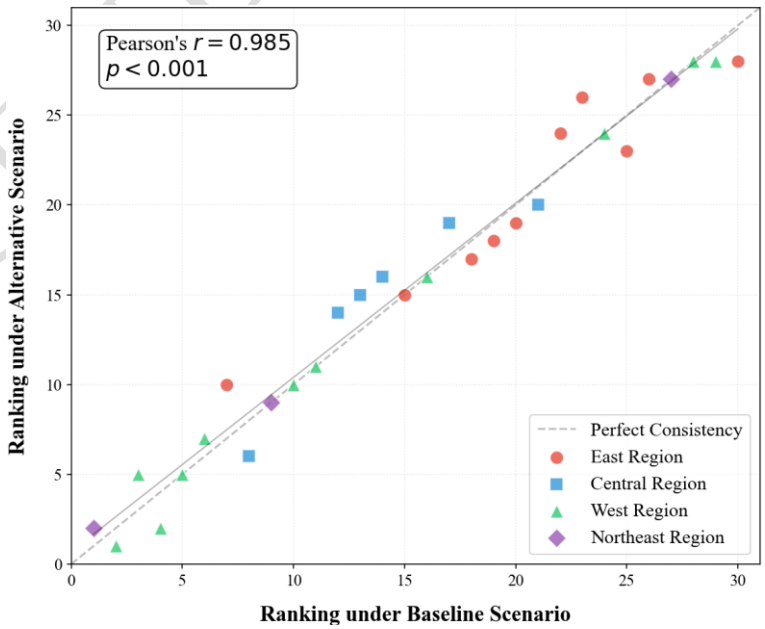

Figure 13. Rank robustness analysis of the CCD under different weighting scenarios

6. Conclusions

6.1 Research Conclusions

This study optimizes the coupled coordination degree (CCD) model and integrates multi-dimensional analysis methods to disclose the temporal and spatial evolution characteristics of the coupling and coordinated development of agriculture and ecological environment in 30 provinces of China during the period from 2013 to 2022. The research results indicate that the level of coupled and coordinated development between these two systems has manifested a marked upward trend, and the synergy effect between the two industries has constantly strengthened. Nevertheless, the issue of uneven coordinated development among regions remains prominent, with the coordinated level in the eastern coastal areas significantly higher than that in the central and western regions. The empirical analysis reveals that the coupled and coordinated development of the two systems possesses significant spatial autocorrelation and exhibits “H-H” and “L-L” agglomeration effects. The hot and cold spot analysis further indicates that the provinces in the eastern coastal areas have become the core regions of coordinated and coordinated development. Meanwhile, the western region has long remained in a state of low coordinated development, and the development bottleneck remains significant. Furthermore, through the analysis of the spatial Markov chain model, it is discovered that the level of regional coordinated and coordinated development has significant path dependence and entrenchment characteristics. The coordinated and coordinated development of the two systems demonstrates a clear “Matthew effect”. In conclusion, although the level of coupling and coordinated development between agriculture and environment has continuously improved nationwide, the regional gap has not yet been fully bridged, and stronger policy intervention and resource integration support are requisite to achieve regional balanced development.

627 *6.2 Policy recommendations*

628 Based on the above empirical findings, the following two targeted policy recommendations are
629 proposed to further enhance the coupling coordination between agriculture and the ecological
630 environment in China:

631 Firstly, in light of the "strong in the east, weak in the west" spatial pattern and pronounced
632 interregional disparities, it is necessary to strengthen regionally differentiated constraints and support
633 at the national level. On the one hand, eastern regions should, while consolidating their advantages
634 in agricultural modernization and environmental governance, place greater emphasis on improving
635 resource-use efficiency and ecosystem stability. They should take the lead in exploring institutional
636 and technological pathways that reconcile green agricultural development with high-level ecological
637 environmental protection, thereby playing a demonstrative and guiding role. On the other hand, fiscal
638 transfers and policy preferences for the central and western regions and parts of the northeast should
639 be increased, with a particular focus on supporting agricultural infrastructure, farmland irrigation and
640 water conservancy, environmental infrastructure, and ecological restoration projects. This would help
641 address weaknesses in green agricultural transition and environmental governance and ease the long-
642 standing "development bottlenecks" associated with persistently low coordination levels.

643 Secondly, Given the pronounced spatial clustering and "Matthew effect" observed in the
644 agriculture–ecological environment coupling coordination level, more closely integrated mechanisms
645 for cross-regional collaborative governance and factor sharing are needed. At the national level,
646 dedicated funds could be established to guide local governments in jointly implementing projects and
647 demonstration programs focused on green agricultural transformation and ecological environmental
648 protection, including the construction of ecological agriculture demonstration zones, integrated river
649 basin governance areas, and cross-regional ecological compensation pilots. At the regional level,

cooperation should be promoted between developed eastern regions and the central, western, and northeastern regions in areas such as green technologies, ecological governance experience, agricultural branding, and market access. Through talent exchange, technology transfer, and joint project development, the endogenous momentum and external support for coordinated agriculture–environment development in less developed regions can be effectively strengthened.

6.3 Theoretical implications

In terms of the measurement of coupling coordination, this paper refines the traditional CCD model by incorporating logarithmic averaging and exponential transformation. These improvements preserve the intuitive nature of the model while enhancing its ability to characterize extreme values and structural disparities, making it better suited to depicting the synergistic relationships within the complex social–ecological system of agriculture and the ecological environment. This provides a more robust evaluation tool for subsequent related research.

In terms of research perspective, this study draws on a long time series for 30 provinces nationwide to systematically reveal the spatiotemporal patterns, regional disparities, and dynamic evolution paths of agriculture–ecological environment coupling coordination. In doing so, it addresses the limitations of existing studies that tend to focus on local areas or static cross-sections and pay insufficient attention to nationwide spatiotemporal evolution, thereby enriching the spatial research perspective on the coordination between agricultural development and the ecological environment.

In terms of analytical framework, this paper integrates Dagum Gini decomposition, spatial autocorrelation analysis, KDE, spatial Markov chains, and MGWR into a coherent methodological system. By examining overall disparities, spatial patterns, dynamic evolution, and driving mechanisms, it constructs a relatively comprehensive analytical framework. The results demonstrate

673 that incorporating spatial analysis and multiscale approaches into the study of coordinated
674 agriculture–environment development has important theoretical value and practical potential.

675 *6.4 Practical implications*

676 The conclusions of this study have several practical implications for government agencies and
677 practitioners:

678 (1) The pronounced regional disparities and spatial clustering patterns indicate that policies for
679 green agricultural development and ecological environmental governance should place greater
680 emphasis on differentiated and targeted interventions, rather than adopting uniform, one-size-fits-all
681 approaches. In the eastern region, priority should be given to enhancing green technology levels and
682 ecosystem stability in order to advance high-quality development. By contrast, the central and western
683 regions and parts of the northeast need to increase investment in improving infrastructure,
684 strengthening ecological carrying capacity, and raising resource-use efficiency.

685 (2) The observed high–high and low–low spatial clusters, together with evident path dependence
686 and the "Matthew effect," provide an important signal to policymakers: the earlier strong
687 interventions are implemented in low-coordination regions to break "low-level lock-in," the lower
688 the long-term governance costs are likely to be. Therefore, when formulating regional plans, major
689 productivity layouts, and ecological conservation redlines, the level of coordinated agriculture–
690 environment development should be treated as a key constraint and evaluation criterion.

691 (3) The spatial analysis results show that geographically adjacent regions exhibit significant
692 interdependence in their agriculture–ecological environment coordination levels. This underscores
693 the need to fully account for spatial spillover and linkage effects in policy design, and to encourage
694 the establishment of cross-jurisdictional platforms for joint governance and information sharing. Such
695 arrangements can enhance policy coherence and improve the efficiency of resource allocation.

6.5 Study limitations

Although this study makes certain explorations in terms of methodology and research perspective, several limitations remain that warrant further refinement in future work. First, despite the optimization of the traditional CCD model, it is still difficult to fully capture all complex nonlinear relationships and feedback mechanisms between agricultural development and the ecological environment, and some potential interaction effects may not be adequately reflected within the present analytical framework. Second, the analysis focuses primarily on interprovincial patterns within China and does not extend to cross-country comparisons or regions at different stages of development, so the external applicability of the conclusions to other national or regional contexts requires further empirical testing.

6.6 Future research

Building on the above limitations, future research can be deepened along several directions. First, subsequent studies may focus more closely on the impacts and underlying mechanisms of external shocks—such as climate change, extreme weather events, public health crises, and international trade frictions—on the coupling coordination degree between the two systems. This would enable a more comprehensive understanding of system resilience and vulnerability under high-risk scenarios. Second, future work could make greater use of high-resolution data, including remote sensing and geospatial big data, as well as micro-level survey data from households and enterprises. Strengthening interdisciplinary integration across economics, geography, ecology, environmental science, and sociology would further support the development of a more systematic theoretical framework and policy system for coordinated development between agriculture and the ecological environment.

Acknowledgments

This study was financially supported by Scientific Research Project of Anhui Provincial Education Department (Grant No. 2025AHGXZK30314).

References

Bao, Q., Yuxin, Z., Yuxiao, W. & Feng, Y. (2020). Can Entropy Weight Method Correctly Reflect the Distinction of Water Quality Indices? *Water Resources Management,* 34. 10.1007/s11269-020-02641-1.

Bianchi, F. J. J. A., Booij, C. J. H. & Tscharntke, T. (2006). Sustainable pest regulation in agricultural landscapes: a review on landscape composition, biodiversity and natural pest control. *Proceedings of the Royal Society B: Biological Sciences,* 273**,** 1715-1727. doi:10.1098/rspb.2006.3530.

Burian, A., Kremen, C., Wu, J. S.-T., Beckmann, M., Bulling, M., Garibaldi, L. A., Krisztin, T., Mehrabi, Z., Ramankutty, N. & Seppelt, R. (2024). Biodiversity–production feedback effects lead to intensification traps in agricultural landscapes. *Nature Ecology & Evolution,* 8**,** 752-760. 10.1038/s41559-024-02349-0.

Cao, L., Li, T., Wang, R. & Zhu, J. (2020). Impact of COVID-19 on China's agricultural trade. *China Agricultural Economic Review,* 13**,** 1-21. 10.1108/caer-05-2020-0079.

Chen, X., Chen, S., He, Z., Xue, D., Fang, G., Pan, K. & Fang, K. (2022). Developing a system for comprehensive regional Eco-environmental quality assessment in mountainous areas—A case study of Western Sichuan, China. *Frontiers in Environmental Science,* 10**,** 879662.

Cheng, C., Zhang, S., Zhou, M., Du, Y. & Ge, C. (2022). Identifying important ecosystem service areas based on distributions of ecosystem services in the Beijing–Tianjin–Hebei region, China. *PeerJ,* 10**,** e13881.

Gallardo, R. K. (2024). The Environmental Impacts of Agriculture: A Review. *International Review of Environmental and Resource Economics,* 18**,** 165-235. 10.1561/101.00000166.

Han, G., Wei, Z., Zheng, H. & Zhu, L. (2024). Evaluation Index System of Rural Ecological Revitalization in China: A National Empirical Study Based on the Driver-Pressure-State-Impact-Response Framework. *Land,* 13**,** 1270. doi:10.3390/land13081270.

He, S. (2019). Research on the Dynamic Mechanisms and Policies for the Synergistic Promotion of Rural Ecological Compensation and Green Development. *Modern Economic Research***,** 106-113. 10.13891/j.cnki.mer.2019.06.017.

Hu, J., Zhang, J. & Li, Y. (2022). Exploring the spatial and temporal driving mechanisms of landscape patterns on habitat quality in a city undergoing rapid urbanization based on GTWR and MGWR: The case of Nanjing, China. *Ecological Indicators,* 143**,** 109333. https://doi.org/10.1016/j.ecolind.2022.109333.

Hu, T., Zhang, X., Khanal, S., Wilson, R., Leng, G., Toman, E. M., Wang, X., Li, Y. & Zhao, K. (2024). Climate change impacts on crop yields: A review of empirical findings, statistical crop models, and machine learning methods. *Environmental Modelling & Software,* 179**,** 106119. https://doi.org/10.1016/j.envsoft.2024.106119.

Huo, T. & Zhang, L. (2025). The Impact of Digital Inclusive Finance on High-Quality Agricultural Development: A Mechanism Analysis from the Perspective of Supply and Demand. *Research on Technology, Economy, and Management***,** 97-103.

Kamalov, F. (2020). Kernel density estimation based sampling for imbalanced class distribution. *Information Sciences,* 512**,** 1192-1201. https://doi.org/10.1016/j.ins.2019.10.017.

Kopittke, P. M., Menzies, N. W., Wang, P., Mckenna, B. A. & Lombi, E. (2019). Soil and the intensification of agriculture for global food security. *Environment international,* 132**,** 105078.

Lee, J. & Li, S. (2017). Extending Moran's Index for Measuring Spatiotemporal Clustering of Geographic Events. *Geographical Analysis,* 49**,** 36-57. https://doi.org/10.1111/gean.12106.

Lei, X. & Kocoglu, M. (2025). When good intentions meet bad outcomes: Evidence from China's cleaner production mandate. *Energy Economics,* 152**,** 109030. https://doi.org/10.1016/j.eneco.2025.109030.

Lei, X. & Kocoglu, M. (2026a). Bad Money drives out good: Peer abnormal R&D intensity and innovation quality. *Economics Letters,* 259**,** 112801. https://doi.org/10.1016/j.econlet.2025.112801.

Lei, X. & Xu, X. (2024). Storm clouds over innovation: Typhoon shocks and corporate R&D activities. *Economics Letters,* 244**,** 112014. https://doi.org/10.1016/j.econlet.2024.112014.

Lei, X. & Zhang, Z. (2026b). The algorithm Can't see everything: Human capital as the hidden variable in environmental technology success. *Journal of Environmental Management,* 397**,** 128287. https://doi.org/10.1016/j.jenvman.2025.128287.

Liang, D., Lu, X., Zhuang, M., Shi, G., Hu, C., Wang, S. & Hao, J. (2021). China's greenhouse gas emissions for cropping systems from 1978–2016. *Scientific Data,* 8**,** 171. 10.1038/s41597-021-00960-5.

Liu, P., Wang, C., Xie, X. & Lu, T. (2025). Study on the Coupling and Harmonization of Agricultural Economy, Population Development, and Ecological Environment in the Yangtze River Basin. *Sustainability,* 17**,** 2209. doi:10.3390/su17052209.

Liu, Y., Sun, D., Wang, H., Wang, X., Yu, G. & Zhao, X. (2020). An evaluation of China's agricultural green production: 1978–2017. *Journal of Cleaner Production,* 243**,** 118483. https://doi.org/10.1016/j.jclepro.2019.118483.

Lundin, O., Smith, H. G., Rundlöf, M. & Bommarco, R. (2013). When ecosystem services interact: crop pollination benefits depend on the level of pest control. *Proc Biol Sci,* 280**,** 20122243. 10.1098/rspb.2012.2243.

Luo, X. (2023). Research on Pathways to Ecological Protection and Modern Agricultural Development in the Yellow River Basin. *China Collective Economy***,** 44-47.

Madjar, R. M., Vasile Scăețeanu, G. & Sandu, M. A. (2024). Nutrient water pollution from unsustainable patterns of agricultural systems, effects and measures of integrated farming. *Water,* 16**,** 3146.

Power, A. G. (2010). Ecosystem services and agriculture: tradeoffs and synergies. *Philosophical Transactions of the Royal Society B: Biological Sciences,* 365**,** 2959-2971. doi:10.1098/rstb.2010.0143.

Qiu, B. & Luo, D. (2021). A Grey Multi-Level Evaluation of Industrial Park Ecology Based on a Coefficient of Variation-Attribute Hierarchy Model. *Sustainability,* 13**,** 1805. doi:10.3390/su13041805.

Raven, P. H. & Wagner, D. L. (2021). Agricultural intensification and climate change are rapidly decreasing insect biodiversity. *Proceedings of the National Academy of Sciences,* 118**,** e2002548117. doi:10.1073/pnas.2002548117.

Rockström, J., Gupta, J., Qin, D., Lade, S. J., Abrams, J. F., Andersen, L. S., Armstrong Mckay, D. I., Bai, X., Bala, G., Bunn, S. E., Ciobanu, D., Declerck, F., Ebi, K., Gifford, L., Gordon, C., Hasan, S., Kanie, N., Lenton, T. M., Loriani, S., Liverman, D. M., Mohamed, A., Nakicenovic, N., Obura, D., Ospina, D., Prodani, K., Rammelt, C., Sakschewski, B., Scholtens, J., Stewart-Koster, B.,

Tharammal, T., Van Vuuren, D., Verburg, P. H., Winkelmann, R., Zimm, C., Bennett, E. M., Bringezu, S., Broadgate, W., Green, P. A., Huang, L., Jacobson, L., Ndehedehe, C., Pedde, S., Rocha, J., Scheffer, M., Schulte-Uebbing, L., De Vries, W., Xiao, C., Xu, C., Xu, X., Zafra-Calvo, N. & Zhang, X. (2023). Safe and just Earth system boundaries. *Nature,* 619**,** 102-111. 10.1038/s41586-023-06083-8.

Sharpe, D. J. & Wales, D. J. (2021). Nearly reducible finite Markov chains: Theory and algorithms. *The Journal of Chemical Physics,* 155. 10.1063/5.0060978.

Shi, Z., Huang, H., Wu, Y., Chiu, Y.-H. & Qin, S. (2020). Climate Change Impacts on Agricultural Production and Crop Disaster Area in China. *International Journal of Environmental Research and Public Health,* 17**,** 4792.

Sj, W., W, K., L, R. & Al, e. (2021). Research on misuses and modification of coupling coordination degree model in China. *JOURNAL OF NATURAL RESOURCES***,** 793. https://doi.org/10.31497/zrzyxb.20210319.

Smith, P., Martino, D., Cai, Z., Gwary, D., Janzen, H., Kumar, P., Mccarl, B., Ogle, S., O'mara, F. & Rice, C. (2008). Greenhouse gas mitigation in agriculture. *Philosophical transactions of the royal Society B: Biological Sciences,* 363**,** 789-813.

Tang, M., Ding, J., Kong, H., Bethel, B. J. & Tang, D. (2022). Influence of Green Finance on Ecological Environment Quality in Yangtze River Delta. *Int J Environ Res Public Health,* 19. 10.3390/ijerph191710692.

Wan, M., Kuang, H., Yang, Y., He, B., Zhao, S., Wang, Y. & Huo, J. (2023). Evaluation of Agricultural Green Development Based on Gini Coefficient and Hesitation Fuzzy Multi-Attribute Decision-Making: The Case of China. *Agriculture,* 13**,** 699. doi:10.3390/agriculture13030699.

Wang, C., Meng, X., Siriwardana, M. & Pham, T. (2022). The impact of COVID-19 on the Chinese tourism industry. *Tourism Economics,* 28**,** 131-152. 10.1177/13548166211041209.

Watson, S. C. L., Newton, A. C., Ridding, L. E., Evans, P. M., Brand, S., Mccracken, M., Gosal, A. S. & Bullock, J. M. (2021). Does agricultural intensification cause tipping points in ecosystem services? *Landscape Ecology,* 36**,** 3473-3491. 10.1007/s10980-021-01321-8.

Wu, H., Ding, B., Liu, L., Zhou, L., Meng, Y. & Zheng, X. (2024). Have Agricultural Land-Use Carbon Emissions in China Peaked? An Analysis Based on Decoupling Theory and Spatial EKC Model. *Land,* 13**,** 585. doi:10.3390/land13050585.

Zhao, M., Xia, T. & Ma, Z. (2022). Research on Evaluating the Synergistic Progress of Ecological Protection and High-Quality Agricultural Development in the Yellow River Basin. *Resources and Environment in the Yangtze Basin,* 31**,** 2096-2107.